Metabolomics (2025) 21:68
https://doi.org/10.1007/s11306-025-02258-8

REVIEW ARTICLE

A narrative review of metabolomics approaches in identifying biomarkers of doxorubicin-induced cardiotoxicity

Amarnath Singh[1] · Maham Bakhtyar[2] · Se-Ran Jun[3] · Marjan Boerma[4] · Renny S. Lan[5] · L. Joseph Su[6] · Sam Makhoul[7] · Ping-Ching Hsu[1]

Received: 12 December 2024 / Accepted: 4 April 2025

Abstract

Background While anthracyclines, commonly used in cancer treatment, are well known to cause cardiotoxicity, no validated biomarkers currently exist that can predict the early development of doxorubicin-induced cardiotoxicity (DIC). Therefore, identifying early biomarkers of DIC is urgently needed. Metabolomics approaches have been used to elucidate this relationship and identified related metabolite markers. However, differences in pre-clinical model systems make it challenging to draw definitive conclusions from the discoveries and translate findings into clinical applications.

Aim of review A systematic literature search on metabolomics studies of DIC was conducted with the goal to identify and compare study results reported using in vitro models, animal models, and studies from clinical patients. Metabolites identified across all studies were pooled to uncover biologically meaningful patterns that are significantly enriched in the data. Finally, pooled metabolites perturbed by DIC were mapped to metabolic pathways to explore potential pathological implications.

Results We reviewed 28 studies published between 2000 and 2024 that utilized metabolomics approaches to investigate DIC. The included studies used a variety of analytical techniques, including LC–MS, GC–MS, and NMR. The analysis revealed that metabolites such as inosine, phenylalanine, arginine, and tryptophan were commonly perturbed across all study models, with carnitine metabolism and purine and pyrimidine metabolism being the most affected pathways. Metabolite Set Enrichment Analysis (MSEA) using MetaboAnalyst identified the arginine biosynthesis, citrate cycle, and alanine, aspartate, and glutamate metabolism pathways as significantly enriched.

Conclusion These findings underscore the potential of metabolomics in identifying early biomarkers for DIC, providing a foundation for future studies aimed at preventing cardiotoxicity and improving treatment strategies for cancer patients receiving DOX-containing therapies.

Key scientific concepts of review Altogether, metabolomics studies suggest metabolic alterations in DIC, albeit little overlap between studies especially with animal and human studies. Attempts at intercepting these pathways have shown that intervention in DIC may be possible. Future research should focus on developing precise cardiotoxicity models that incorporate cancer metabolism, as these will be crucial in bridging the gap between laboratories (in vitro and animal models) and clinical studies to identify subclinical biomarkers in the early stage of DIC that can effectively identify new targets for interventions to reduce lethal cardiovascular disease risk.

Keywords Metabolomics · Cardiotoxicity · Doxorubicin

✉ Ping-Ching Hsu
PHsu@uams.edu

[1] Department of Environmental Health Sciences, Fay W. Boozman College of Public Health, University of Arkansas for Medical Sciences, Little Rock, AR, USA

[2] Department of Internal Medicine, College of Medicine, University of Arkansas for Medical Sciences, Little Rock, AR, USA

[3] Department of Biomedical Informatics, University of Arkansas for Medical Sciences, Little Rock, AR, USA

[4] Department of Pharmaceutical Sciences, University of Arkansas for Medical Sciences, Little Rock, AR, USA

[5] Department of Pediatrics, College of Medicine, University of Arkansas for Medical Sciences, Little Rock, AR, USA

[6] Peter O'Donnell Jr. School of Public Health, UT Southwestern Medical Center, Dallas, TX, USA

[7] CARTI Research Department, Little Rock, AR, USA

Published online: 17 May 2025

1 Introduction

With rapid advances in the quality of health care and cancer treatment, there has been an improvement in the 5-year overall survival with most cancers (Allemani et al., 2018; Anderson et al., 2021). Among cancer treatments, anthracycline-based chemotherapies, especially doxorubicin (DOX), are a widely used and fundamental treatment in reducing mortality rates for breast cancer and other malignancies.

Despite its effectiveness, the use of DOX is significantly limited by dose-dependent cardiotoxicity, with a notable 26% incidence of heart failure observed at cumulative doses of 550 mg/m^2 (Chatterjee et al., 2010; Deidda et al., 2019; Feijen et al., 2019; Takemura & Fujiwara, 2007; Vejpongsa & Yeh, 2014). Acute cardiotoxicity affects up to 11% of patients, while chronic cardiotoxicity occurs in approximately 1.7% of cases (Yeh & Bickford, 2009). Acute cardiotoxicity is considered reversible, and presents with chest pain, palpitations, or tachycardia, which may result from supraventricular or ventricular arrhythmias, atrioventricular heart block, or myopericarditis (Camilli et al., 2024; Cardinale et al., 2015; Gawlik et al., 2023; Totzeck et al., 2023). Patients at the extremes of ages are more prone to developing irreversible chronic cardiotoxicity, which presents with clinical signs of heart failure (HF) (Heemelaar et al., 2023). The onset of HF with dyspnea, fatigue, orthopnea, third heart sound (S3), and a reduced left ventricular ejection fraction (LVEF) portends a poor prognosis (Chatterjee et al., 2010). Patients initiated with DOX-based regimens are monitored for cardiotoxicity with echocardiography, multigated acquisition scan, cardiac magnetic resonance (CMR), or radionuclide ventriculography. However, echocardiography is operator-dependent (Gottdiener et al., 2004), and there are risks associated with radiation exposure from radionuclide angiography (Volkova & Russell, 2011). The use of CMR is limited due to the technology and expertise required (Qin et al., 2022). Endomyocardial biopsy is the gold standard for determining cardiotoxicity after chemotherapy, but the invasiveness and sampling error limit its use (Palaskas et al., 2021; Saidi & Alharethi, 2011).

Several studies have shown that changes in metabolic pathways occur long before the onset of clinical symptoms or changes in LVEF (Cocco et al., 2020; Planek et al., 2020; Schnackenberg et al., 2016). However, no validated biomarkers that can predict the early development of drug-induced cardiotoxicity currently exist. Cardiac troponin T and troponin I have been used in preclinical studies to assess early cardiac tissue damage (Hausner et al., 2013); but, their predictive value in cardiotoxicity is limited and has not been validated in clinical studies (Herman et al., 1998; Monsuez, 2012; Yu et al., 2018).

Early biomarkers of DOX-induced cardiotoxicity (DIC) are urgently needed to identify patients at risk. Metabolomics uses mass spectrometry (MS) and/or nuclear magnetic resonance (NMR) spectroscopy to identify perturbations in low molecular weight metabolites resulting from toxicity and disease (Patti et al., 2012; Viant et al., 2019), and is ideally suited for identifying early indications of DIC (Clish, 2015). It is a relatively new field that has rapidly emerged as an indispensable tool for precision medicine in identifying alteration in metabolic pathways (Srivastava, 2019). Modern advances in analytical technology, particularly metabolomics, present an opportunity to identify early biomarkers of DIC. Early detection of these biomarkers would allow healthcare providers to intervene before clinical symptoms develop, potentially preventing or minimizing cardiac damage in patients (Yuan et al., 2020; Zhang et al., 2021).

1.1 Aim of review

This narrative review with systematic search approach aimed to compile and analyze the literature on the use of metabolomics to assess DIC in different model systems, including findings from in vitro systems, animal models, and human studies, and to summarize metabolite markers of DIC in order to identify knowledge gaps in the field. Markers identified from different model systems were further extrapolated in metabolic pathways associated with DIC to shed light on how the knowledge gained can be translated into clinical studies, ultimately helping to develop targeted treatment strategies for chemotherapy-induced cardiotoxicity.

2 Methods

2.1 Literature search

We systematically searched the PubMed database for studies that used metabolomics approaches to investigate DIC. The bibliographic search was performed in September 2024 and included literature from the year 2000 up to that time. An English language filter was applied due to limited translation resources. We used the following search terms in PubMed and received the following results: (1) “Metabolomics AND Cardiotoxicity AND Doxorubicin” (n = 44); (2) “Metabolomics AND Doxorubicin” (n = 207); (3) “Metabolic profiling AND Cardiotoxicity AND Doxorubicin” (n = 43); (4) "Untargeted Metabolic profiling AND Cardiotoxicity AND Doxorubicin" (n = 6); (5) "Targeted Metabolic profiling AND Cardiotoxicity AND Doxorubicin" (n = 17).

2.2 Eligibility criteria

In this study, we only included original publications. Reviews and meta-analyses, comments, guidelines, editorials or letters, conference summaries, cardiac toxicity not addressed and non-longitudinal studies were excluded. From the results of the initial query, we filtered based on the following inclusion criteria: (1) studies investigating cardiotoxicity in the context of doxorubicin as part of the treatment; (2) studies employing either targeted or untargeted metabolomics approaches; (3) studies conducted using human subjects, in vivo models, or in vitro systems.

2.3 Data collection process and analysis

AS screened all the article titles and abstracts. Disagreements were resolved by consensus among AS, and PCH. Full texts of articles deemed potentially eligible during the initial screening were obtained for further reading. The search and selection processes are detailed in the flow diagram (Fig. 1).

We searched for overlapping manuscripts from sources (1) to (5) (Sect. 2.1). Out of 317 initially identified manuscripts, 187 duplicates were removed, leaving 130 for further review. These manuscripts, focused on metabolomics and cardiotoxicity, were sorted by relevance, including those investigating the metabolomics aspects of chemotherapy-induced cardiotoxicity. We excluded articles that were unrelated to the topic (n = 36), unrelated to doxorubicin-induced cardiotoxicity metabolomics (n = 18), unrelated to cardiotoxicity (n = 12), did not use doxorubicin as part of cancer treatment (n = 8); and review articles (n = 26). Thirty reports were assessed for eligibility, of which two studies using cyclophosphamide as chemotherapy agent were excluded, and finally the search has led to a total of 28 articles for the final analysis (Table 1 and Supplemental Table 1).

We categorized the available data into three broad groups: studies conducted in 1) in vitro cell culture systems, 2) animal models (mice and rats), and 3) patients. Metabolites with significant alterations in response to DOX identified in the 28 selected articles were summarized and used for pathway enrichment analysis with using MetaboAnalyst 5.0 (Pang et al., 2021). Briefly, all 462 metabolites reported across the 28 studies were pooled into MetaboAnalyst 5.0 to retrieve their corresponding Human Metabolome Database (HMDB) IDs, along with identifiers from Public Chemical Database (PubChem), Chemical Entities of Biological Interest (ChEBI), METLIN Metabolite and Chemical Entity Database (METLIN), and Kyoto Encyclopedia of Genes and Genomes (KEGG). Among these, 231 metabolites were successfully matched to HMDB IDs and subsequently mapped to KEGG human metabolic pathways for functional interpretation. Metabolite Set Enrichment Analysis (MSEA) was conducted using the hypergeometric test to identify biologically meaningful patterns significantly enriched in pre-defined metabolite sets described in the literature. Similarly, we performed separate MSEA analyses for each model system (in vitro, rat, mouse, human) using a list of perturbed metabolites mapped with HMDB IDs to identify both shared and unique metabolic pathways affected across different model systems.

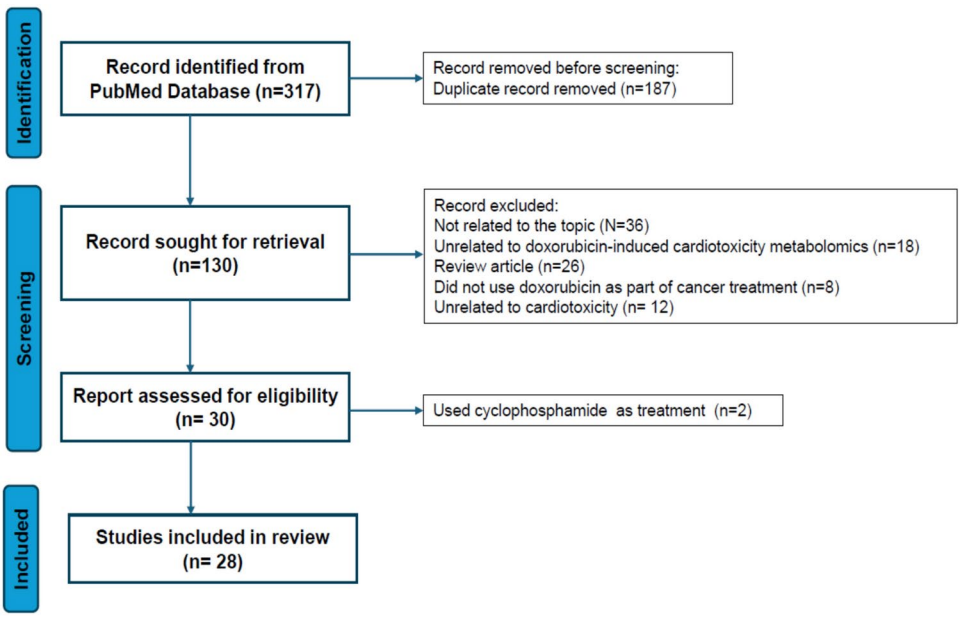

Fig. 1 Flowchart of the literature search and study selection for the narrative review on metabolomics in models of doxorubicin-induced cardiotoxicity

Table 1 Summary of the 28 metabolomics studies on DOX-induced cardiotoxicity included in this review

Sample type	Sample size	Technique	Targeted/ Untargeted metabolomics	Significant metabolites	References
In vitro *studies*					
H9c2 rat cardiomyocytes	NA	UHPLC-MS	Untargeted	5-Methylthioadenosine, Cranitine, Guanosine, Monophosphate, 5-Methyltetrahydrofolate, 5-Thymidylic Acid, S-Adenosylmethionine, Cytidine Monophosphate, N-Acetylneuraminic Acid, 5'-Methylthioadenosine, S-Adenosylhomocysteine, Tryptophan, Methionine, Cytosine, Arginine, Uracil, Uridine, Pantothenic Acid, Inosine, Aspartic Acid, Lysine, Inosinic Acid, Proline, Phenylalanine, Tyrosine, Glutamate, Glutathione, Citrate, Cytidine, Deoxyinosine, Pipecolic, Acid, Betaine, Adenine, N-Acetyl Muramic Acid, Patothenic Acid, S-Adenosylhomocyteine, S-Asenosylmethionine, 5-Methylthioadenosine, Glutamine, 3-Hydroxymethylglutaric Acid, Carnitine	Yi et al. (2018)
Human induced pluripotent stem cell-derived cardiomyocytes	NA	NMR	Targeted	Acetate, Pyruvate, Formate	Chaudhari et al. (2017)
H9c2 rat cardiomyocyte	NA	UHPLC-QTOF-MS	Untargeted	1, 4-beta-D-Glucan, 3-Carboxy, 1-Hydroxypropylthiamine, Diphosphate, 3-Methoxy,4-Hydroxyphenylglycol Glucuronide, Eicosanoyl-CoA, Coenzyme A, Palmitic Acid, Pantothenic Acid, Oleic Acid	Wen et al. (2020b)
Animal studies					
Male C57BL/6 mice	N = 36 (Serum)	UHPLC-QTOF-MS	Untargeted	1-Arachidonoylglycero Phosphoinositol, 8-HOTE, LysoPA(18:1/0:0), LysoPA(18:2/0:0), LysoPA(20:2/0:0), LysoPE (22:5/0:0), PC(15:1/0:0), PC(17:1/0:0), PI(22:6/0:0), PI(18:2/0:0), 15-HPETE, 1-Pentadecanoyl-Glycero-3-Phosphate, 8-HETrE, 20-HDoHE, LysoPC(17:0/0:0), Cer(d18:0/14:0), Cer(d18:0/12:0), LysoPE(22:0/0:0), LysoPE(20:5/0:0), LysoPE(20:4/0:0), LysoPE(20:3/0:0), LysoPE(18:3/0:0), LysoPE(18:2/0:0), LysoPE(18:1/0:0), LysoPE(16:0/0:0), 1-Octadecylglycero-3-Phosphocholine, LysoPE(18:0/0:0), LysoPC(22:5/0:0), LysoPC (20:5/0:0), LysoPC (20:2/0:0), LysoPC (20:1/0:0), LysoPC (20:0/0:0), LysoPC (20:0/0:0), LysoPC (18:3/0:0), LysoPC (18:2/0:0), LysoPC (18:0/0:0), LysoPC (16:1/0:0), LysoPC (16:0/0:0), LysoPC (15:0/0:0), LysoPC (14:0/0:0), LysoPA (18:0/0:0), 9,10-DHOME, 15-HETE, Eicosatrienoic Acid, LysoPC (18:1/0:0), Docosahexaenoic Acid, Eicosapentaenoic Acid, Docosapentaenoic Acid, Phosphorylcholine, Arachidonic Acid, Tryptophan, Uric Acid, L-Phenylalanine, Glycerophosphocholine	Wang et al. (2020)
Male B6C3F1 mice	N = 74 (Heart tissue)	GC–MS, NMR	Targeted	Acetylcarnitine (C2), Acetylornithine, Carnitine, Glutarylcarnitine (C5-DC), Hexenoylcarnitine (C6:1), Pimelylcarnitine (C7-DC), Putrescine, Tryptophan, Citrulline, Valine, Methionine, Leucine, Kynurenine, Arginine, Serotonin, Ornithine, Serine, Lysine, Histidine, Isoleucine, Asparagine, Threonine, Proline, Alanine, Phenylalanine, Tyrosine, Glycine	Schnackenberg et al. (2016)

Table 1 (continued)

Sample type	Sample size	Technique	Targeted/ Untargeted metabolomics	Significant metabolites	References
Male B6C3F1 mice	N = 74 (Plasma)	GC–MS, NMR	Targeted	Acetylornithine, Butyrylcarnitine (C4), Carnitine, Glutaconylcarnitine (C5:1-DC), Glutarylcarnitine (C5-DC), Hexadecadienylcarnitine (C16:2), Hexadecanoylcarnitine (C16), Hydroxyhexadecadienylcarnitine (C16:2-OH), Hydroxyhexadecenoylcarnitine (C16:1-OH), Hydroxyoctadecenoylcarnitine (C18:1-OH), Hydroxytetradecenoylcarnitine (C14:1-OH), Nonaylcarnitine (C9), Octadecanoylcarnitine (C18), Pimelylcarnitine (C7-DC), Propionylcarnitine (C3), Tetradecanoylcarnitine (C14), Valerylcarnitine (C5), Tryptophan, Citrulline, Valine, Hydroxyproline, Methionine, Leucine, Glutamine, Arginine, Succinate, Ornithine, Lactate, Serine, Isoleucine, Threonine, Proline, Alanine, Phenylalanine, Tyrosine, Glutamate, Glycine	Schnackenberg et al. (2016)
ICR mice	N = 24 (Heart tissue)	GC–MS	Untargeted	Glyceraldehyde 3-phosphate, Linoleic Adid, β-Hydroxybutyric acid, Dihydroxyacetone phosphate, Phosphate, Arachidonic Acid, Threonic Acid, Valine, Stearic Acid, Fructose, Glutamine, Succinate, Myo-Inositol, Lactate, Isoleucine, Threonine, Proline, Alanine, Phenylalanine, Malate, Glycine, Glucose, Citrate, Cholesterol	Tan et al. (2011)
Male BALB/c mice	N = 30 (Serum)	UHPLC-QTOF-MS	Untargeted	Cer(d18:0/22:0), Cer(d18:0/20:0), Cer(d18:0/18:0), Cer(d18:0/16:0),Cer(d18:0/14:0), Sphingosine, Linoleyl carnitine, Palmitoylcarnitine, Propionylcarnitine, Proline, Valine, PC (34:2), Creatine, SM(d18:1/24:2), SM(d18:2/24:0), SM(d18:1/22:0), SM(d18:1/16:0), LysoPC(22:6), LysoPC(20:5), LysoPC(18:3), Arginine, Lysine	Zhang et al. (2021)
Male Sprague–Dawley rats	N = 24 (Serum)	GC–MS	Untargeted	11-Eicosanoic Acid, 9-Octadecenamide, Valine, Urea, Aspartate, Lactate, Proline, Alanine, D-Galactose, D-Glucose	Alhazzani et al. (2021)
Male Sprague–Dawley rats	N = 16 (Heart tissue)	GC–MS	Untargeted	MG (16:0/0:0/0:0), 3-Methyl-1-Pentanol, Lactate, Valine, Stearic Acid, Propanoic Acid, Phenol, Palmitic Acid, Alanine, Glycerol, Glycine, D-Glucose, Cholesterol	Geng et al. (2021)
Male Sprague–Dawley rats	N = 16 (Serum)	GC–MS	Untargeted	Tyrosine, MG (16:0/0:0/0:0), MG (0:0/18:0/0:0), Oleamide, N-Methylphenylethanolamine, Lactate, Tryptophan, Valine, Stearic Acid, Leucine, Urea, Pyroglutamate, Palmitic Acid, Serine, Isoleucine, Proline, Alanine, Glutamate, Glycine, D-Glucose, Cholesterol	Geng et al. (2021)
Male Wistar rats	N = 35 (Plasma)	UHPLC-QTOF-MS	Targeted	Linoleic Acid, Alpha-Ketogluterate, Cartolone-3-Glucoronide, Ecosapentaenoic Acid, L-Palmitoyl Carnitine, LysoPC(18:1 (11Z)/0:0), LysoPC(20:4 (8Z,11Z,14Z,17Z)/0:0), LysoPE (0:0/24:6 (6Z,9Z,12Z,15Z,18Z,21Z)), Tetradecanefioic Acid, Pyroglutamine, 11,14,17-Eicosatrienoic Acid, 12,13-Epoxy-9,15-Octadecadienoic Acid, Trimethoprim, Prolylhydroxyproline, Tryptophan, Octanoylcarnitine, Glutamine, Sphingosine, Phenylpyruvic Acid, Tyrosine, Creatine	Yuan et al. (2020)
Male Sprague–Dawley rats	N = 40 (Serum)	UHPLC-QTOF-MS	Untargeted	Acetylphosphate, LysoPC(18:1(9Z)), Oleic acid, Coenzyme A, 3-Carboxy-1-hydroxypropylthiamine diphosphate, PC (16:0/16:0), PE(O-18:1(1Z)/20:4(5Z,8Z,11Z,14Z)), Palmitic acid	Wen et al. (2020c)
Male Sprague–Dawley rats	N = 48 (Serum)	GC/LC–MS	Untargeted	11–12-Epoxyeicosatrienoic Acid, Arachidonic Acid, Linoleylcanitine, Pamitoylcarnitine, Prostaglansin J2, Sphinganine 1-Phsophate, LysoPC (20:2), LysoPC (15:0), LysoPC (14:0), Oleoylcarnitine, Tryptophan, Stearoylcarnitine, Phenylacetylglycine, Hippuric Acid, Indoxyl Sulfate, Linoleic Acid, Cholic Acid, Uric Acid, Sphingosine 1-Phosphate, Taurine, Palmitic Acid, Oleic Acid, Isoleucine, Phenylalanine, Glycocholic Acid, Carnitine	(Zhou et al. (2020)

Table 1 (continued)

Sample type	Sample size	Technique	Targeted/ Untargeted metabolomics	Significant metabolites	References
Male Sprague–Dawley rats	N = 50 (Serum)	UHPLC-QTOF-MS	Untargeted	Arachidonic acid, Phosphatidylethanolamine, Biotinyl-5-AMP, PA (16:0/16:0), Beta-D-Glucuronoside, Hexanoyl-CoA, 15(S)-HETE, Leukotriene D4	Wen et al. (2020a)
Male Sprague–Dawley rats	N = 26 (Heart tissue)	NMR	Untargeted	Alanine, Fumarate, Glycerin, Glycerophosphocholine, Creatine, Carnitine	Niu et al. (2016)
Male Sprague–Dawley rats	N = 26 (Serum)	NMR	Untargeted	3-Hydroxybutyrate, Lipid, N-Acetyl-Glycoprotein, O-Acetyl-Glycoprotein, B-Glucose, Acetone, Phosphocholine, Trimethylamine-N-Oxide, Valine, Leucine, Succinate, Pyruvate, Myo-Inositol, Lactate, Lysine, Isoleucine, Phenylalanine, Glutamate, Formate, Glycerin, Glycine, Citrate, Dimethylglycine, Creatine, Acetoacetate	Niu et al. (2016)
Male Sprague–Dawley rats	N = 60 (Heart tissue)	GC–MS and UPLC-MS/MS	Untargeted	1,3-Dipalmitoylglycerol, 15-Methylpalmitate, 2-Palmitoleoylglycerophosphocholine, 2-Stearoylglycerol (2-Monostearin), Adenosine 5'-Monophosphate (AMP), C-Glycosyltryptophan, Cytidine 5'-Monophosphate (5'-CMP), Decanoyl Sulfate, Glutathione Oxidized (GSSG), Palmitoleate (16:1N7), Riboflavin (Vitamin B2), Sedoheptulose-7-Phosphate, Succinylcarnitine, 2-Linoleoylglycerophosphocholine, 1-Stearoylglycerophosphoglycerol, Phenol Sulfate, N-Acetylmethionine, 1-Oleoylglycerophosphoethanolamine, Palmitoyl Sphingomyelin, Stachydrine, 3-Hydroxydecanoate, Malonylcarnitine, Butyrylcarnitine, Coenzyme A, Nicotinamide, Thiamin Diphosphate, Dehydroascorbate, Citrulline, Stearoylcarnitine, Salicylate, Propionylcarnitine, Octanoylcarnitine, Hexanoylcarnitine, Isovalerylcarnitine, Kynurenine, 3-Indoxyl Sulfate, Uracil, Xanthine, Squalene, Pantothenic Acid, Acetylcarnitine, Anserine, Histidine, Alanine, Glutamate, Glycerate, Glucose, Cytidine, Cholesterol, Carnosine	Chen et al. (2015)
Male Wistar rats	N = 90 (Heart tissue)	NMR	Untargeted	3-Hydroxybutyrate, Acetoacetate, β-Glucose, Dimethyl Glycine, Nicotinamide, Valine, Leucine, Glutamine, Pyroglutamate, Succinate, Taurine, Inosine, Aspartate, Lactate, Lysine, Isoleucine, Asparagine, Alanine, Phenylalanine, Tyrosine, Hypoxanthine, Glutamate, Formate, Fumarate, Fumarate, Glycerol, Glycine, Choline, Creatine, AMP	Andreadou et al. (2014)
Male Wistar rats	N = 42 (Heart tissue)	NMR	Targeted	Alanine, Glutamate, Glutamine, Succinate, Acetate, Creatine, Taurine	Andreadou et al. (2009)
Male Wistar rats	N = 32 (Serum)	UHPLC–MS	Untargeted	Deoxyadenosine, 4-Hydroxy-d-proline, Norvaline, 2-Methylbutyryl glycine, 9'-Carboxy-gamma-tocotrienol, 9-Retinoic acid, Sphingosine 1-phosphate, LysoPE(20:4/0:0),LysoPE(20:3(5Z,8Z,11Z)/0:0), LysoPE(0:0/18:3(6Z,9Z,12Z)), 10,11-dihydro-20-dihydroxy-LTB4, Octadecanedioic acid, PE(20:3(5Z,8Z,11Z)/22:0), Docosapentaenoic acid, SM(d18:1/23:0)	Zhao et al. (2021)
Male BALB/c mice	N = 96 (Serum)	NMR	Untargeted	3-Hydroxybutyrate, 4-Hydroxybutarate, Aspartete, Acetone, Glycylproline, Methionine, Cysteine, Creatinine, Arginine, 5-Hydroxylysine, UDP-glucose, 2-Oxoglutarate, Lactate, Isoleucine, Glutamate, Carnosine, 2-Hydroxybutyrate	Quan Jun et al. (2017)
C57BL/6 J mouse	N = 34 (Heart tissue)	UHPLC-QTOF-MS	Untargeted	SM(d17:2/16:0), SM(d18:1/15:0), LysoPI (18:2), LysoPI (20:4), LysoPE (22:6), LysoPE (22:5), LysoPE (20:3), LysoPE (18:1), LysoPE (14:0), LysoPE (16:1), Tetradecanoylcarnitine, Eicosadienoic Acid, Docosatrienoic Acid, Leukotriene B4, Ethanolamide, Dodecanoylcarnitine, Arachidonic Acid, Linoleic Acid, Xanthine, Uric Acid, Sphingosine 1-Phosphate, Succinate, Isoleucine, Malate	Ding et al. (2023)

Table 1 (continued)

Sample type	Sample size	Technique	Targeted/ Untargeted metabolomics	Significant metabolites	References
Swiss albino mice	N = 30 (Heart tissue)	LC–MS/MS	Targeted	1-Palmitoyl-2- (5-Hydroxy-8-Oxo-6-Octenedioyl)-Sn-Glycero-3-Phosphatidylcholine, 1-Stearoyl-2-Hydroxy-Sn-Glycero-3-Pe, 5-Hydroxy-DL-Tryptophan, Adenosine Monophosphate (AMP), Palmitoyl Carnitine, 3-Hydroxyoctadecanoylcarnitine, Linoleamide, Leukotriene B4, Taurine, Testosterone, D-Pantothenic Acid, Choline, Creatine	Khan et al. (2022)
Male Wistar rats	N = 18 (Heart tissue)	LC–MS	Targeted	3-Phosphoglycerate And 2-Phosphoglycerate, 6-Bisphosphate, C10:0 Carnitine, C10:1 Carnitine, C12:0 Carnitine, C12:1 Carnitine, C14:0 Carnitine, C14:1 Carnitine, C14:2 Carnitine, C16:0 Carnitine, C16:1 Carnitine, C16:2 Carnitine, C18:0 Carnitine, C18:1 Carnitine, C6:0 Carnitine, C8:0 Carnitine, C8:1 Carnitine,, Carnitine, Fructose-1-Phosphate, Glucose-6-Phosphate, Fructose-6-Phosphate, C18:2 Carnitine, ATP, Phosphoenolpyruvate, Succinate, Lactate, Glucose	Thonusin et al. (2023b)
Male Wistar rats	N = 18 (Serum)	LC–MS	Targeted	C10:0 Carnitine, C10:1 Carnitine, C12:0 Carnitine, C12:1 Carnitine, C14:0 Carnitine, C14:1 Carnitine, C14:2 Carnitine, C16:0 Carnitine, C16:1 Carnitine, C16:2 Carnitine, C18:0 Carnitine, C18:1 Carnitine, C6:0 Carnitine, C8:0 Carnitine, C18:2 Carnitine, Succinate, Carnitine, Acetoacetate	Thonusin et al. (2023b)
Male Wistar rats	N = 24 (Serum)	UHPLC-QTOF-MS	Targeted	C14:0 carnitine, C18:2 carnitine, Lysine, C16:2 carnitine, Arginine, PA(36:2), PI(38:4), LysoPC(18:0), C14:1 Carnitine, PE(38:4), Histidine, PG(34:1), LysoPE(20:0), C18:1 carnitine, PG(36:2), PG(36:1), C16:0 carnitine, PC(38:6), C14:2 carnitine, PE(38:2), C2:0 carnitine, PE(38:6), LysoPS(18:0), C10:1 carnitine, PI(36:2), PI(36:1), Ornithine, Uracil, PC(34:1), PC(36:2), Phenylalanine, Succinate, Valine, Citrulline, N-Acetylornithine, Taurine, Glutamine, Tyrosine, 2,3-DihydroxybenzoateM, Hypoxanthine, PC(34:2), C5:0 carnitine, Methionine, LysoPC(18:2), Tryptophan, Homocysteic acid, Uridine, Alpha-Ketoglutarate, Threonine, Acetic acid, Acetoacetate, Palmitoleic acid, C4:0 carnitine, PE(34:1), Aspartate, Asparagine, PG(38:1), Citrate, PC(36:4)	Thonusin et al. (2023a)
Male Wistar rats	N = 24 (Heart tissue)	UHPLC-QTOF-MS	Targeted	C4:0 carnitine, PC(36:2), PE(36:3), C2:0 carnitine, Glutamate, PG(38:1), PE(36:2), Taurine, C12:1 carnitine, C16:2 carnitine, PE(38:2), C10:1 carnitine, N-Acetylornithine, PC(34:2), C8:1 carnitine, PC(36:1), PE(36:1), C16:0 carnitine, C18:2 carnitine, Tryptophan, LysoPC(18:2), C5:0 carnitine, C14:1 carnitine, C16:1 carnitine, Hypoxanthine, PE(38:4), LysoPE(18:0), Citrulline, Alanine, Uridine, Glutamine, PA(36:1), PE(34:1), PC(34:1), Homocysteic acid, C18:1 carnitine, Histidine, PC(36:4), LysoPI(18:1), LysoPE(20:2), Ornithine, PS(36:2), Choline, LysoPC(16:0), LysoPE(18:1), C12:0 carnitine, PA(36:2), LysoPE(16:0), C8:0 carnitine, LysoPC(18:1), Acetoacetate, Lactate, Stearic acid, PG(36:2), PI(34:1), LysoPI(18:0), Tyrosine, PS(40:6), PS(38:4), Oleic acid, Malate, Glycine, Proline, Threonine, PI(38:4), Valine, Isoleucine, Alpha-ketoglutarate, Asparagine, PG(34:1), Serine, PI(36:1), Phenylalanine, Arachidonic acid, Methionine, Linoleic acid, Aspartate, Palmitic acid, PC(38:6), LysoPE(20:0), PG(36:1), PE(38:6), C14:0 carnitine, Lysine, LysoPS(18:0), C18:0 carnitine, Arginine, Citrate, 2,3-Dihydroxybenzoate, Myristic acid, C3:0 carnitine	Thonusin et al. (2023a)

Table 1 (continued)

Sample type	Sample size	Technique	Targeted/ Untargeted metabolomics	Significant metabolites	References
ICR mice	N = 48 (Serum)	UHPLC-QTOF-MS	Untargeted	12-Hydroxy-12- Octadecanoylcarnitine, Tetradecenoylcarnitine, Alpha-Ketoglutarate, LysoPI(20:4), Palmitoleoylcarnitine, MG(0:0/16:0/0:0), 3-Oxododecanoic Acid, 3-Oxodecanoic Acid, LysoPC(22:6), LysoPC(20:4), LysoPC(20:1), LysoPC(20:0), LysoPC(18:3), Arachidonoylcarnitine, Tetradecanoylcarnitine, Dodecanoylcarnitine, 3-Hydroxycapric Acid, Docosahexaenoic Acid, Prostaglandin E2, Arachidonic Acid, Taurochenodesoxycholic Acid, L-Pipecolic Acid, Hexanoylglycine, Kynurenine, Glutamine, Deoxycholic Acid, Arginine, 3-Hydroxydodecanoic Acid, Sphinganine, Succinate, Palmitoylcarnitine, Ornithine, Phenylpyruvic Acid, Acetylcarnitine, Lactate, Lysine, Histidine, Proline, Tyrosine, Glycerophosphocholine, Carnitine	Xue et al. (2023)
C57BL/6 mice	N = 18 (Serum)	LC–MS/MS	Targeted	Cer 16:0, Cer 22:2, Cer 23:0, Cer 24:0 OH, Cer 24:1, Cer 24:2	Yun et al. (2021)
Clinical patients					
Human	N = 38 (Plasma)	LC–MS	Targeted	Citrate, Inosine, Hypoxanthine, Aconitic acid, Uric acid, Pseudouridine, Orotic acid	Asnani et al. (2020)
Human	N = 170 (Plasma)	LC- MS/MS	Targeted	Arginine, asymmetric dimethylarginine, N-monomethylarginine	Finkelman et al. (2017)
Human	N = 74 (Plasma)	UHPLC-QTOF-MS	Targeted	Dodecenoylcarnitine, Hexadecadienoylcarnitine, Isoleucine Leucine, Lysophosphatidylcholine (16:0), Lysophosphatidylethanolamine (18:1), Lysophosphatidylinositol (18:1), Oleoylcarnitine, Phosphatidic Acid (34:1), Phosphatidylcholine (36:1), Phosphatidylcholine (36:2), Phosphatidylethanolamine (34:1), Phosphatidylethanolamine (38:4), Phosphatidylglycerol (34:1), Phosphatidylglycerol (36:1), Phosphatidylglycerol (36:2), Phosphatidylserine (38:4), Phosphatidylserine (40:6), Tetradecadienoylcarnitine, Tetradecenoylcarnitine, Myristoylcarnitine, Linoleylcarnitine, Palmitoleoylcarnitine, Lauroylcarnitine, Arachidonic Acid, Tryptophan, Stearoylcarnitine, Propionylcarnitine, Octanoylcarnitine, Hexanoylcarnitine, Isobutyrylcarnitine, Isovalerylcarnitine, Decanoylcarnitine, Glutamine, Palmitoylcarnitine, Acetylcarnitine, Phenylalanine, Malate, Glycine	Thonusin et al. (2024)

UHPLC Ultra high-pressure liquid chromatography, *MS* mass spectrometry, *GC* gas chromatography, *LC* liquid chromatography, *NMR* nuclear magnetic resonance, *HPLC* high performance liquid chromatography, *HILIC* hydrophilic interaction liquid chromatography, *UHPLC-QTOF-MS* ultra high-pressure liquid chromatography, quadrupole time-of-flight mass spectrometry, *QQQ-MS/MS* triple-quadrupole tandem mass spectrometry, *BCAA* branched-chain amino acids

3 Results

Twenty-eight studies were eligible and included in the final review. In animal models, because metabolic similarities between rats and humans are higher than between mice and humans (Blais et al., 2017; Gibbs et al., 2004; Mattes et al., 2014), rat models were the most commonly studied and comprised 14 articles. A total of 8 studies used mouse models, 3 used in vitro cell culture models, and 3 were patient-based studies. The studies are detailed in Sect. 3.2 below.

3.1 Methods in metabolic profiling and statistical analyses

Metabolic profiling was conducted using various techniques, including gas chromatography (GC) / liquid chromatography (LC)-MS (1 study), GC–MS (3 studies), GC–MS; ultra-performance liquid chromatography (UPLC)-MS/MS (1 study), LC–MS (2 studies), LC–MS/MS (4 studies), LC–MS/MS and NMR combined (1 study), NMR alone (4 studies), ultra-high pressure liquid chromatography (UHPLC)-MS (2 studies), and UHPLC– quadrupole time-of-flight (QTOF)-MS (10 studies). A total of 17 studies identified potential

biomarkers through untargeted metabolomics, while 11 studies employed targeted metabolomics. Various statistical methods were used, including univariate t-tests, one-way analysis of variance (ANOVA), machine learning algorithms such as Principal Component Analysis (PCA), Partial Least Squares (PLS), or Orthogonal projections to Latent Structures Discriminant Analysis (OPLS-DA) with Variable Importance in Projection (VIP) to identify aberrant metabolites. Software tools such as SIMCA-P and the web-based platform MetaboAnalyst (https://dev.metaboanalyst.ca/home.xhtml) were used, and KEGG Pathway database was referenced in the pathway analysis. Metabolites identified from the 28 studies included in this review are summarized in Table 1 and Supplemental Table 1.

3.2 Summary of the main results and findings

3.2.1 In vitro cell culture studies

Traditionally, animal model studies have been used for toxicological risk assessment; however, recent advances have made cell culture studies invaluable for providing a well-controlled environment to investigate the molecular basis of toxicity.

Among the three studies using cell culture systems, Chaudhari et al. (2017) examined cultures of human-induced pluripotent stem cell-derived cardiomyocytes (hiPSC-CMs), followed by H-NMR-based metabolic profiling to investigate DOX-induced toxicity. Of the 20 targeted metabolites, significant changes were observed in pyruvate, acetate, and formate. Repeated exposure to DOX resulted in reduced acetate and pyruvate uptake, as well as decreased ATP production, indicating dysfunctional mitochondrial energy metabolism. The irreversible depletion of formate was hypothesized to result from disrupted nucleotide metabolism (Chaudhari et al., 2017).

Wen et al. (2020b) investigated the potential cardioprotective effects of higenamine (HG) combined with [6]-gingerol ([6]-GR) on chronic heart failure induced by DOX in H9c2 rat cardiomyocyte cell lines. This systematic review primarily focused on the adverse cardiac effects of DOX compared to the control group, rather than the protective efficacy of the combined treatments. A significant perturbation of metabolites was observed in H9c2 cells treated with DOX, compared to the control group, based on metabolite ratios. Specifically, the study found a significant decrease in the levels of eight metabolites: 1,4-beta-D-Glucan, 3-carboxy-1-hydroxypropylthiamine diphosphate, 3-Methoxy-4-Hydroxyphenylglycol glucuronide, Eicosanoyl-CoA, Coenzyme A, palmitic acid, pantothenic acid, and oleic acid (Table 1) (Wen et al., 2020b). Pre-treatment with HG, [6]-GR, or their combination shifted metabolic parameters towards control levels, with the HG/[6]-GR combination showing the strongest therapeutic effect. While [6]-GR alone had a weaker impact, the HG/[6]-GR combination demonstrated superior efficacy in regulating DOX-induced metabolic disorders compared to individual treatments.

Similarly, Yi et al. (2018) examined the protective effects of the traditional Chinese medicine Danhong against DOX-induced toxicity in H9c2 cells. Using non-targeted metabolomics via LC–MS, they identified 31 altered metabolites in DOX-treated cells (Table 1) (Yi et al., 2018), mainly related to disturbances in amino acid and nucleotide metabolism. In DOX-treated cells, significant alterations in amino acid profiles were observed, including decreased levels of lysine, tyrosine, phenylalanine, tryptophan, and methionine. These amino acids are crucial for energy metabolism and are precursors for substances that enter the citrate cycle, such as pyruvate, 2-oxoglutarate, and fumarate. This metabolic disruption likely contributes to the energy deficiency and heart damage caused by DOX. Additionally, abnormalities in nucleotide metabolism, particularly in purine and pyrimidine pathways, were noted in the DOX group. The downregulation of nucleotides like adenine, cytidine, uridine, and inosine suggests an inhibition of cell proliferation, likely due to impaired DNA and RNA synthesis. However, Danhong treatment was found to modulate key metabolic pathways, including those involving arginine, glutathione (GSH), pantothenic acid, cytidine, inosine, and 5'-methylthioadenosine. The results suggest that Danhong injection may exert therapeutic effects by improving energy metabolism and reducing oxidative stress.

3.2.2 Mouse model studies

Animal studies have been used for centuries as a human proxy to untangle the complexity of metabolic pathways, drug efficacy, and toxicity.

Schnackenberg et al. (2016) conducted a targeted metabolomics study to examine the cumulative effects of DOX administered weekly at 3 mg/kg for eight weeks in the heart and plasma of male B6C3F1 mice. Myocardial injury and cardiac pathology were observed at cumulative DOX doses of 6, 9, 12, 18, and 24 mg/kg. At a 6 mg/kg dose, 37 plasma metabolites and 22 heart tissue metabolites showed significant increases, while 5 heart metabolites—primarily carnitines, including acetylcarnitine (C2), carnitine (C0), glutarylcarnitine (C5-DC), hexenoylcarnitine (C6:1), and pimelylcarnitine (C7-DC) decreased compared to the control group (Supplemental Table 1 and Table 1). By the end of the 8-week study, a consistent and significant reduction in the levels of arginine, acetylornithine, carnitine, and acetylcarnitine was observed in cardiac tissue, along with a persistent elevation in succinate and acetate levels. These

metabolic changes were significant at the 6 mg/kg dose and occurred prior to any alterations in troponins or cardiac function, suggesting their potential as early biomarkers for predicting cardiotoxicity (Schnackenberg et al., 2016).

Tan et al. (2011) identified 24 prospective myocardial metabolite biomarkers from myocardial tissue of ICR mice treated with a single dose of DOX (20 mg kg^{-1}) using GC–MS. Of the 24 metabolites identified via an untargeted approach, 8 metabolites (linoleic acid, β-hydroxybutyric acid, arachidonic acid, L-valine, lactate, isoleucine, threonine, and citrate) decreased, while 16 metabolites, including glyceraldehyde 3-phosphate (G-3-P), dihydroxyacetone phosphate (DHAP), phosphate, threonic acid, stearic acid, fructose, glutamine, succinate, myo-inositol, proline, l-alanine, phenylalanine, malate, glycine, glucose, and cholesterol, increased in the DOX-treated group (Table 1 and Supplemental Table 1) (Tan et al., 2011). The authors concluded that elevated levels of fructose, glucose, G-3-P, and DHAP were linked to increased glycolysis, while reduced lactate was attributed to upregulated myocardial lactate dehydrogenase. The reduction in citrate, along with elevated levels of malate and succinate, suggested a disturbance in the citric acid cycle. Regarding lipid metabolism, elevated stearic acid levels indicated reduced β-oxidation of saturated fatty acids. Additionally, the reduction in valine and isoleucine was hypothesized to result from their utilization as an alternative energy source (Tan et al., 2011).

To investigate the cardioprotective effects of dexrazoxane (DZR) in the setting of DIC, Quan Jun Y. et al. used a flank tumor model of CT26 colorectal carcinoma cells (cell injection on day 0). A total of 96 male BALB/c mice were divided into tumor and non-tumor bearing and treated with 12 mg kg^{-1} DOX per day on days 8, 11 and 14. In the DOX-treated tumor-bearing mice, 1H-NMR spectroscopy analysis of serum revealed increased levels of 2-oxoglutarate, VLDL/LDL, 3-hydroxybutyrate, 5-hydroxylysine, 4-hydroxybutyrate, 2-hydroxybutyrate, creatine, and arginine, while levels of acetone, glutamate, lactate, cysteine, isoleucine, aspartate, UDP-glucose, glycylproline, methionine, and carnosine were decreased. To isolate the effect of DOX and eliminate the confounding impact of cancer, the DOX-treated control mice were compared with control mice, revealing increases in 4-hydroxybutyrate, trans-4-hydroxy-L-proline, 5-hydroxylysine, alanine, 2-hydroxybutyrate, 2-oxoglutarate, 3-hydroxybutyrate, and creatine, with decreases in glucose, glutamate, acetoacetate, acetone, TMAO, cysteine, aspartate, isoleucine, and glycylproline levels (Supplemental Table 1). These changes were observed in the serum using ^{1}H-NMR spectroscopy, compared with control mice, suggesting enhanced oxidation (QuanJun et al., 2017).

Hydrophilic Interaction Liquid Chromatography (HILIC) is used to separate polar compounds. Recently, Zhang et al. (2021) used this technique to assess the potential benefit of pretreatment with *Astragalus* polysaccharides (ASP) for 3 days, followed by DOX (3 mg kg^{-1} per day on days 1, 5, 9 and 11) in 30 male BALB/c mice. In the DOX-treated group, perturbations in 22 polar serum metabolites were observed compared to the control group. Of these, 9 metabolites, including sphingomyelin, phosphatidylcholine, propionyl carnitine, lysine, arginine, and proline, were decreased, while 13 metabolites, such as lysophosphatidylcholine, ceramide, valine, sphingosine, creatine, palmitoylcarnitine, and linoleylcarnitine, were increased (Supplemental Table 1) (Zhang et al., 2021). Notably, 12 of these metabolites, which are involved in sphingolipid and glycerophospholipid metabolism, showed reversal in the ASP pretreatment group (Zhang et al., 2021).

Ding et al. (2023) screened multiple mitochondria-targeted components from Sini decoction (SND) to explore their potential therapeutic effects against DOX-induced cardiomyopathy (DCM) in male C57BL/6 J mice. Using a novel cardiac mitochondrial membrane chromatography (CMMC)-TOFMS system, the authors detected DOX-induced alterations in 23 metabolites using an untargeted approach. In the DOX-treated group, 13 metabolites including sphingomyelin, lysophosphatidylinositol, lysophosphatidylethanolamine, eicosadienoic acid, linoleic acid, xanthine, and malic acid—were decreased, while 10 metabolites including tetradecanoylcarnitine, docosatrienoic acid, leukotriene B4 ethanolamide, dodecanoylcarnitine, arachidonic acid, uric acid, sphingosine 1-phosphate, succinic acid, and isoleucine were increased (Supplemental Table 1) (Ding et al., 2023). Most of these metabolites are associated with arachidonic acid metabolism, citrate cycle metabolism, and fatty acid metabolism.

To investigate the cardioprotective effects of administering DOX in conjugates with green synthesized selenium nanoparticles (SeNPs) in Swiss albino mice, Khan et al. (2022) divided animals into 6 groups (n = 5 per group) treated intraperitoneally: control, SeNP1 (0.5 mg/kg), SeNP2 (1.5 mg/kg), DOX (5 mg/kg), or the conjugates SeNP1-DOX (5 mg/kg), or SeNP2-DOX (7 mg/kg) (Khan et al., 2022). Mice received DOX injections every other day for 7 days. Using LC–MS/MS metabolomics, they found DOX treatment decreased 6 metabolites (linoleamide, leukotriene B4, taurine, testosterone, choline, creatine) and increased 7 metabolites (5-hydroxy-DL-tryptophan, AMP, palmitoyl carnitine, 3-hydroxyoctadecanoylcarnitine, D-pantothenic acid, etc.) in heart tissue (Supplemental Table 1 and Table 1). Notably, the SeNP-DOX conjugate reversed several of these DOX-induced metabolic disturbances, suggesting that SeNPs can mitigate DOX toxicity.

These findings position the SeNP-DOX conjugate as a promising therapeutic strategy for reducing DOX's adverse effects.

In the study by Xue et al. (2023), untargeted metabolomics was used to investigate the combination effects and mechanisms of the Huangqi-Fuzi herb-pair (Qifu decoction, QFD) against DIC in mice. Forty-eight male ICR mice (25-28 g) were randomly divided into six groups (n = 8): control, DOX, QFD-low dosage (QFD-L), QFD-high dosage (QFD-H), HQD, and FZD. The DOX group received intraperitoneal injections of 3 mg/kg every other day for two weeks (cumulative dose 21 mg/kg). The QFD-L, QFD-H, HQD, and FZD groups were orally administered their respective treatments at doses of 4.5 g, 9 g, 6 g, and 3 g of crude herbs/kg body weight for 14 consecutive days. The untargeted metabolomics approach identified 41 metabolites downregulated in the DOX group compared to control (Supplemental Table 1 and Table 1) (Xue et al., 2023). DOX disrupted 12 metabolic pathways, including energy metabolism, amino acid metabolism, arachidonic acid metabolism, and glycerophospholipid metabolism. QFD significantly regulated all 12 pathways, demonstrating stronger cardioprotective effects compared to the individual herbs. These findings suggest that QFD's synergistic effects in maintaining metabolic homeostasis make it a promising therapeutic option for DIC.

3.2.3 Rat model studies

Rat models present distinct advantages over mice as research models: their larger physical size simplifies surgical interventions and sample collection, while their easier handling improves the accuracy of blood sampling and imaging procedures. Most importantly, rat metabolism better resembles human metabolic processes, making them particularly valuable for studying human diseases and drug responses (Bryda, 2013).

Geng et al. (2021) investigated the metabolic derangements in the serum, heart, liver, kidney, and brains tissues of male Sprague–Dawley (SD) rats after exposure to DOX. The rats were randomly divided into a control and DOX group. A total of 7 doses of 2.5 mg/kg were injected intraperitoneally every two days, while the control group was injected with normal saline Perturbations, 21, 13, 9, 9, and 7 dysregulated metabolites were observed in serum, heart, liver, brain, and kidney respectively between the DOX and the control groups. In the heart, the authors observed increased levels of L-valine, phenol, glycine, D-glucose, and cholesterol were observed, while decrease in levels of monoacyl glyceride (MG) (16:0/0:0/0:0), 3-methyl-1-pentanol, D-lactic acid, stearic acid, propanoic acid, palmitic acid, L-alanine, and glycerol were observed (Supplemental Table 1 and Table 1) (Geng et al., 2021). Similarly, in serum samples increased levels of 15 metabolites (pyroglutamic acid, L-serine, L-isoleucine, L-proline, L-glutamic acid, glycine, D-glucose and cholesterol) and decreased levels of 6 metabolites (MG (16:0/0:0/0:0), MG (0:0/18:0/0:0), D-lactic acid, stearic acid, palmitic acid, L-alanine) were observed (Supplemental Table 1 and Table 1). Commonly dysregulated metabolites in serum and heart tissue such as MG (16:0/0:0/0:0), D-lactic acid, stearic acid, palmitic acid, L-alanine, L-valine, glycine, D-glucose, cholesterol) could serve as important biomarkers(Geng et al., 2021).

Niu et al. (2016) studied metabolic perturbations in heart, serum, urine, and kidney of 26 male SD rats after intraperitoneal administration of DOX for 15 days. The rats were divided into a DOX group (n = 16) and a control group (n = 10). DOX was administered intraperitoneally on alternate days for 15 days at a successively increasing dose of 1, 1, 2, 2, 3, 3, 4, and 4 mg/kg. Significant metabolic changes were observed in the DOX-treated group compared to control group, with 13 metabolites (pyruvate, succinate, creatine, dimethylglycine, glycerin, isoleucine, leucine, lysine, myo-inositol, N-acetyl-glycoprotein, O-acetyl-glycoprotein, phenylalanine) showing increased levels, while 12 metabolites showing decreased levels in serum (3-hydroxybutyrate, acetoacetate, acetone, citrate, formate, glutamate, glycine, lactate, etc.) (Niu et al., 2016). In the heart, seven metabolites were elevated (carnitine, glutamine, glycerophosphocholine, inosine, taurine, uridine, etc.), while histidine and lactate were reduced. At the end of the study period, echocardiographic measurements showed significant reductions in the thickness of the intraventricular septum in systole, the left ventricular posterior wall in diastole, and fractional shortening in the DOX-treated group, correlating with these metabolic shifts. Serum metabolites like 3-hydroxybutyrate, glycine, and acetone, and heart metabolites like carnitine and fumarate were key markers. The study identified fatty acid metabolism disruption as a key factor in DIC (Niu et al., 2016).

Yun et al. (2021) assessed the cardioprotective effects of periplocymarin against DOX-induced heart failure in mice. Male C57BL/6 mice (8–10 weeks old) were divided into three groups: control (n = 5), DOX (n = 7), and DOX + periplocymarin (n = 6). The DOX+periplocymarin group received periplocymarin (5 mg/kg) for 3 days, followed by a single DOX injection (20 mg/kg) to induce heart failure. Periplocymarin treatment continued for 3 days after the DOX injection, while control and DOX groups received saline injections. Targeted metabolomics revealed increases in all six ceramide metabolites in the DOX group compared to controls (Supplemental Table 1 and Table 1), with ceramides linked to cardiac dysfunction via apoptosis, oxidative

stress, and inflammation, ultimately culminating in heart failure (Yun et al., 2021).

Zhao et al. (2021) examined the cardioprotective effects of captopril and Schisandrin B (Sch B) on DOX-induced myocardial injury in male Wistar rats. The rats were divided into four groups (control, model, Captopril, and Sch B), with the model group receiving DOX injections (2.5 mg/kg) for 6 weeks to induce myocardial injury. The Sch B (10 mg/kg) and Captopril (2.25 mg/kg) groups were treated for 2 weeks after DOX administration (Zhao et al., 2021). Using UHPLC-MS, the study identified 15 potential metabolites in serum samples of the DOX group compared to the control, including 4 decreased metabolites (e.g., 9'-carboxy-gamma-tocotrienol, docosapentaenoic acid) and 11 increased metabolites (e.g., sphingosine 1-phosphate, deoxyadenosine, SM(d18:1/23:0)) (Supplemental Table 1 and Table 1). Lipid metabolites reflect biochemical pathways involved in energy metabolism, lipid signaling, oxidative stress, and inflammation– processes crucial for maintaining heart health and potentially signaling cardiac dysfunction (Bhat et al., 2024; Borodzicz-Jażdżyk et al., 2022; Foran et al., 2024; Schulze et al., 2016).

Zhou et al. (2020) explored the cardioprotective effects of Sini Decoction (SND) on DOX-induced heart failure in rats. Forty-eight male Sprague–Dawley rats were divided into six groups: control, DOX, SND + DOX, ACFD + DOX, ZOFD + DOX, and GUFD + DOX. SND and other treatments were administered daily at 10 g/kg for three weeks, while DOX (2.5 mg/kg) was administered intraperitoneally over 2 weeks to induce heart failure (Zhou et al., 2020). Untargeted metabolomic analysis using GC-LC–MS revealed 7 downregulated metabolites (including 11–12-epoxyeicosatrienoic acid, LysoPC (20:2), hippuric acid, indoxyl sulfate, taurine, isoleucine, and carnitine) and 19 upregulated metabolites (such as arachidonic acid, linoleylcarnitine, palmitoylcarnitine, LysoPC(15:0), LysoPC(14:0), linoleic acid, sphingosine 1-phosphate, palmitic acid, phenylalanine, and glycocholic acid) in the DOX-treated group compared to controls. These metabolic alterations reflect the cardiotoxic effects of DOX, likely involving disruptions in lipid metabolism, amino acid metabolism, and oxidative stress pathways. The metabolomic analysis highlights potential biomarkers and metabolic pathways implicated in DIC, offering possible targets for cardioprotective interventions.

Yuan et al. (2020) employed integrated metabolomics and proteomics of cardiac tissue and plasma to investigate the molecular mechanisms underlying DIC in male Wistar rats (Yuan et al., 2020). The study revealed decreased levels of 12 metabolites (including alpha-ketoglutarate, cartolone-3-glucuronide, eicosapentaenoic acid, glutamine, L-octanoylcarnitine, pyroglutamine, tryptophan, and tyrosine), and increased levels of 9 metabolites (such as 11,14,17-eicosatrienoic acid, 12,13-epoxy-9,15-octadecadienoic acid, alpha-linolenic acid, LysoPC(18:1 (11Z)/0:0), phenylpyruvic acid, and sphingosine) in the DOX-treated group compared to controls (Supplemental Table 1 and Table 1). They identified 21 biomarkers related to tyrosine, tryptophan, phenylalanine biosynthesis, D-glutamine, D-glutamate metabolism, and fatty acid biosynthesis. The study suggests that DOX-induced heart failure (HF) involves disruptions in energy, amino acid, fatty acid, and glycerolipid metabolism. While healthy hearts primarily rely on fatty acid oxidation, failing hearts shift toward glucose oxidation, a change linked to hypertrophy and impaired function.

Andreadou et al. (2014) studied the cardioprotective effects of oleuropein in a chronic model of DIC in rats (Andreadou et al., 2014). The rats were divided into six groups and treated with DOX, oleuropein, or a combination of both. The study identified 28 upregulated metabolites, including fumarate, glutamate, glutamine, glycerol, glycine, hypoxanthine, inosine, and isoleucine, along with one downregulated metabolite, acetoacetate/acetone in DOX compared to controls (Supplemental Table 1 and Table 1). DOX treatment significantly impaired left ventricular contractility induced inflammatory and degenerative lesions, and increased oxidative stress markers such as malondialdehyde, interleukin-6, and endothelin-1. DOX also disrupted nitric oxide (NO) homeostasis by increasing inducible nitric oxide synthase (iNOS) expression while reducing endothelial nitric oxide synthase (eNOS), Akt, and AMP-activated protein kinase (AMPK) activation. Metabolomic analysis showed altered energy metabolism and protein biosynthesis in DOX-treated rats, whereas oleuropein mitigated these adverse effects. In addition, studies in the human prostate cancer cell line PC-3 showed that oleuropein did not alter DOX-induced cancer cell growth inhibition in vitro. The study concluded that oleuropein prevents DIC by activating AMPK, reducing iNOS expression, and restoring NO bioavailability, suggesting it as a potential therapeutic strategy to prevent DIC.

Chen et al.(2015) conducted a metabolomic study to examine DIC and the cardioprotective effects of Shengmai Injection (SMI) in male Sprague–Dawley rats (Chen et al., 2015). The rats were randomized into a control group, DOX treatment (6 injections, 2.5 mg/kg each, over 2 weeks), SMI treatment (12 injections, 3 ml/kg each, over 4 weeks), or DOX and SMI. Metabolic profiling was performed using GC–MS and LC–MS/MS, revealing 26 downregulated metabolites in heart tissue, including 3-indoxyl sulfate, acetylcarnitine, AMP, carnosine, citrulline, dehydroascorbate, glutamate, glycerate, histidine, and malonylcarnitine, as well as 24 upregulated metabolites such as hexanoylcarnitine, isovalerylcarnitine, kynurenine, and α-acetylmethionine in

the DOX group compared to controls. The study demonstrated that DIC led to significant cardiac remodeling, dysfunction, and metabolic disturbances, particularly in lipid, amino acid, vitamin, and energy metabolism. SMI treatment improved cardiac function, reduced fibrosis, apoptosis, and oxidative stress, and restored energy metabolism, highlighting its cardioprotective potential. These findings indicate that SMI confers cardioprotection by enhancing energy metabolism, reducing oxidative stress, and modulating key metabolic pathways.

Thonusin et al. (2023a) investigated serum metabolomes as potential non-invasive biomarkers and therapeutic targets for DOX- and trastuzumab-induced cardiotoxicity in male Wistar rats. The rats were divided into four groups: control, doxorubicin, trastuzumab, and their respective vehicle groups (Thonusin et al., 2023a). Metabolomic analysis was performed using MS, revealing significant alterations in 107 serum metabolites (e.g., histidine, homocysteic acid, hypoxanthine, lysine, LysoPC(18:0), LysoPC(18:2), methionine, N-acetylornithine, and ornithine) and 100 cardiac metabolites (e.g., N-acetylornithine, ornithine, PA(36:1), PA(36:2), PC(34:1), 2,3-dihydroxybenzoate, acetoacetate, alpha-ketoglutarate, arachidonic acid, and arginine) (Supplemental Table 1 and Table 1). The study assessed the relationship between 100 cardiac metabolites and 107 serum metabolites to understand the associations of these metabolites with doxorubicin-induced cardiotoxicity (DIC). The analysis revealed strong correlations between 72 cardiac and 61 serum metabolites in the doxorubicin (DOX) treatment group. DOX treatment caused more pronounced changes in cardiac function and injury markers compared to trastuzumab, indicating greater cardiotoxicity. The study emphasizes the potential of blood metabolomic profiling as a non-invasive approach for assessing heart failure severity and underscores the possibility of developing metabolic-targeted therapies to prevent or mitigate cardiotoxicity.

3.2.4 Human studies

A case–control study by Asnani et al. (2020) involving 38 female breast cancer patients found that decreased plasma levels of citric acid at 3 months after starting DOX correlated with changes in LVEF. The study targeted 71 metabolites representing various metabolic pathways and defined cardiotoxicity as a reduction in LVEF of ≥ 10% or a decrease to < 55% relative to baseline. Among patients who developed cardiotoxicity by six months, increases in purine and pyrimidine metabolites and decreases in citric acid and aconitic acid levels were observed (Asnani et al., 2020).

In a study of 170 breast cancer patients, Finkelman et al (2017) investigated six pre-selected plasma metabolites—arginine, citrulline, ornithine, asymmetric dimethylarginine, symmetric dimethylarginine, and N-monomethylarginine—at baseline, one month, and two months following DOX-containing chemotherapy to explore the link between oxidative/energy metabolites and DIC. Of the 170 patients, 32 developed acute cardiotoxicities over a maximum follow-up period of 5.4 years. One-month post-chemotherapy, decreased plasma arginine levels were associated with DIC, while two months post-chemotherapy, increased levels of asymmetric dimethylarginine and N-monomethylarginine were associated with acute cardiotoxicity (Finkelman et al., 2017).

Thonusin et al. (2024) investigated changes in peripheral blood plasma metabolomes as potential markers for the severity and prognosis of DIC in breast cancer patients, with a focus on differences between HER2-positive and HER2-negative patients. The study included 37 HER2-positive and 37 HER2-negative breast cancer patients, assessing cardiac function. Significant changes in blood metabolomes were observed between HER2-positive and HER2-negative patients two weeks post-DOX treatment (Thonusin et al., 2024). Specifically, 33 metabolites were altered in HER2-positive patients, while 29 metabolites were altered in HER2-negative patients (Supplemental Table 1 and Table 1). These changes were associated with disruptions in amino acid, fatty acid, and phospholipid metabolism. The study also found correlations between plasma metabolome changes and cardiac parameters, such as LVEF and cardiac injury biomarkers, suggesting that plasma metabolomes could serve as markers of DIC severity. Furthermore, in HER2-negative patients, changes in blood metabolomes two weeks after treatment were predictive of long-term cardiac outcomes, highlighting their potential as prognostic markers. These findings suggest that plasma metabolome analysis may offer non-invasive markers for assessing DIC severity and prognosis, with the possibility to tailor metabolic interventions based on HER2 status.

3.3 Significantly perturbed metabolites were identified across three major model systems (in vitro, animal, human)

The studies summarized above utilized various sample types, including cell lines, plasma, serum, and heart tissue from both animal and humans (Fig. 2a). A total of 28 studies were included in the analysis, leading to the identification of five common metabolites (citrate, inosine, phenylalanine, arginine, and tryptophan) that were shared across all three model types (Fig. 2a). Between animal and human studies, 27 common perturbed metabolites were identified, primarily linked to carnitine metabolism, purine and pyrimidine metabolism, and tryptophan metabolism. In cell line and animal studies, 22 metabolites were identified, including the

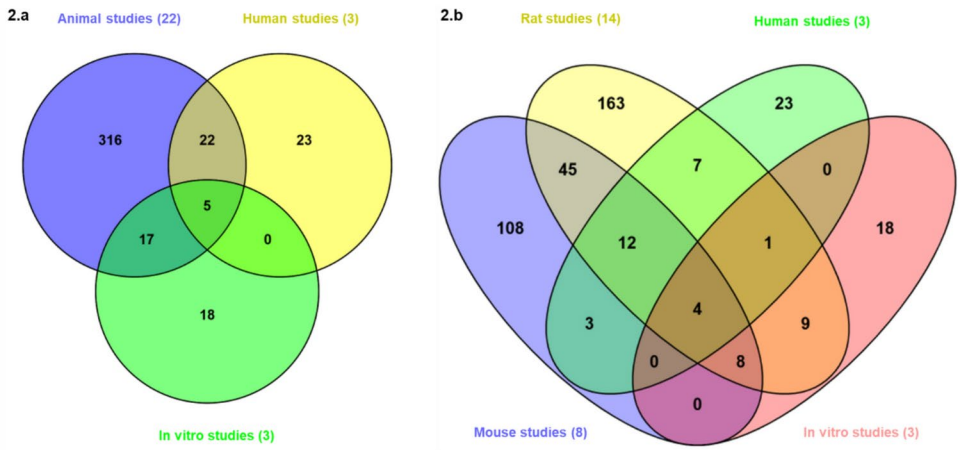

Fig. 2 Venn diagrams representing overlapping significantly perturbed metabolites across different study models. **a** Overlap of significantly altered metabolites in response to DOX doxorubicin-induced cardiotoxicity (DIC) in in vitro, animal, and human studies; **b** Overlap of significantly altered metabolites in response to DOX in vitro, rat, mouse, and human studies

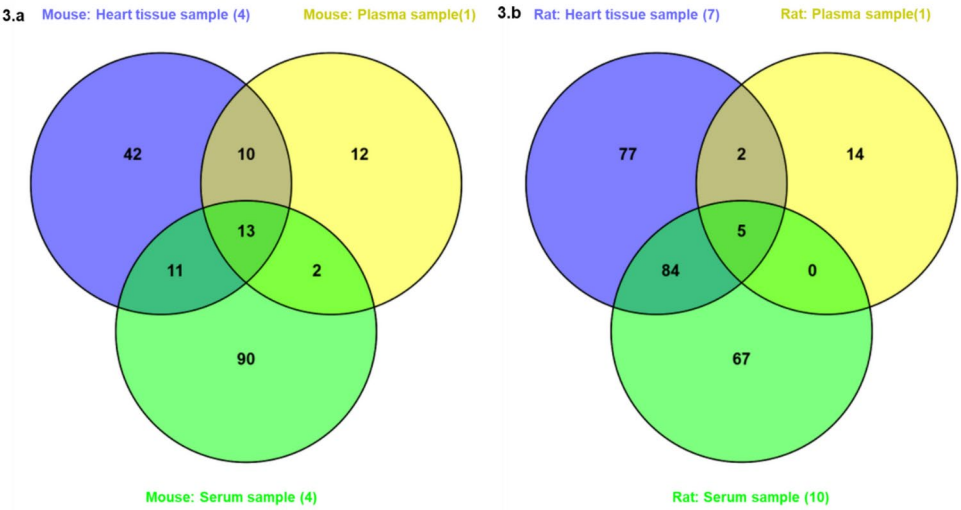

Fig. 3 Venn diagram representing overlapping significantly perturbed metabolites across different sample types in mice and rat Studies. **a** Overlap of significantly altered metabolites due to DIC in mice across heart tissue, serum, and plasma samples. **b** Overlap of significantly altered metabolites due to DIC in rats across heart tissue, serum, and plasma samples

five shared metabolites across all models (Fig. 2a). These metabolites were predominantly involved in amino acid, purine, and pyrimidine metabolism.

3.4 Comparison of significantly perturbed metabolites in the in vitro, rat, mouse, and human studies

In a deeper comparison of different animal models (rat and mouse) with in vitro and human studies, citrate, phenylalanine, arginine, and tryptophan were the most significantly perturbed metabolites (Fig. 2b). Specifically, acetic acid, cytidine, formate, inosine, palmitic acid, uridine, uracil, coenzyme A, oleic acid, pyruvate were metabolites commonly affected in the animal models and in vitro studies (Fig. 2b). For details on their regulation, please refer to Supplemental Table 1″. Between rat and human studies, carnitine metabolites (such as stearoylcarnitine, octanoylcarnitine, hexanoylcarnitine, isovalerylcarnitine, and acetylcarnitine) were the most affected (Fig. 2b). Notably, between rat and mouse studies, 69 common perturbed metabolites were identified, including valine, proline, pantothenic acid, carnitine, glutamate, tyrosine, aspartate, kynurenine, 3-hydroxybutyrate alanine, succinate, taurine, LysoPC, LysoPE, acetylcarnitine and others. Most of these metabolites were associated with alanine, aspartate and glutamate metabolism; phenylalanine, tyrosine and tryptophan biosynthesis; and glycine, serine, and threonine metabolism.

3.5 Significantly perturbed metabolites in heart tissue, plasma, and serum samples in mice

Eight studies using mice as model systems were included, focusing on different sample types: four on heart tissues, one on plasma samples, and four on serum samples. Notably, Schnackenberg et al. (2016) conducted a study that included both plasma and heart tissue samples. Across the studies, the most significantly perturbed metabolites identified in heart tissue, plasma, and serum samples included phenylalanine, lactate, succinate, glutamine, tetradecanoylcarnitine, carnitine, ornithine, arginine, methionine, valine, and tryptophan (Fig. 3a). In heart tissue and serum samples,

24 perturbed metabolites were identified, including palmitoylcarnitine, uric acid, arachidonic acid, dodecanoylcarnitine, eicosadienoic acid, LysoPE (22:5/0:0), LysoPI (20:4), lysine, acetylcarnitine, and kynurenine, along with 13 metabolites common across all three sample types (Fig. 3a). In heart tissue and plasma samples, 23 shared metabolites were observed, including glycine, alanine, serine, tyrosine, threonine, leucine, citrulline, acetylornithine, glutarylcarnitine (C5-DC), and pimelylcarnitine (C7-DC), in addition to the 13 metabolites common across all three sample types. Similarly, 15 metabolites were consistent across plasma and serum samples, including glutamate and C3:0 carnitine, along with the same 13 metabolites common across all three sample types (Fig. 3a). These findings suggest that heart tissue, plasma, and serum are reliable sample types for studying DIC. Importantly, isoleucine, lactate, proline, tryptophan, valine, methionine, arginine, and ornithine, which were consistently identified across all three sample types, may serve as key biomarkers for DIC.

3.6 Significantly perturbed metabolites in heart tissue, plasma, and serum samples in rats

In rats, alpha-ketoglutarate, glutamine, creatine, tyrosine, and tryptophan were the most significantly perturbed metabolites across heart tissue, plasma, and serum samples (Fig. 3b). Comparisons between heart tissue and serum samples identified 89 commonly perturbed metabolites, predominantly belonging to amino acid metabolites, carnitine metabolites, and phospholipid metabolites, which were the most frequently observed categories (Fig. 3b). Interestingly, five metabolites overlapped between plasma and serum samples, while two metabolites, linoleic acid and octanoylcarnitine, overlapped between plasma and heart tissue.

This systematic review identified and summarized significant metabolites consistently reported across multiple studies in heart tissue, serum, plasma, and cell lines, with a focus on metabolites identified in at least two studies (Fig. 4). The most prominently upregulated metabolites across multiple studies and sample types include phenylalanine, succinate, glycine, valine, glutamine, tyrosine, tryptophan, leucine, lactate, isoleucine, alanine, threonine, taurine, proline, palmitoylcarnitine, and methionine. In contrast, consistently downregulated metabolites include glutamate, C10:1 carnitine, carnitine tryptophan, lactate, arginine, alanine, tryptophan, proline, citrate, arachidonic acid, and C18:1 carnitine.

3.7 Metabolite set enrichment analysis

We pooled all 462 metabolites identified from all 28 studies into MetaboAnalyst 5.0, and further used MSEA to identify biologically meaningful patterns that are significantly enriched in the data. MSEA has a built-in tool to convert between compound common names, synonyms,

Metabolites	Up	Down	Metabolites	Up	Down	Metabolites	Up	Down	Metabolites	Up	Down
15-HETE	0	2	Carnitine	2	6	Lactate	5	6	Palmitoylcarnitine	4	2
2,3-Dihydroxybenzoate	2	0	Carnosine	0	2	Leucine	6	0	Palmitoleic Acid	1	1
3-Hydroxybutyrate|	2	1	Cer(d18:0/14:0)	1	1	Linoleic Acid	3	2	Palmitoleoylcarnitine	1	1
Acetic Acid	2	1	Cholesterol	4	0	Linoleylcarnitine	3	0	Pantothenate	0	3
Acetoacetate	3	2	Choline	2	1	Lysine	4	4	PC(34:1)	1	1
Acetone	0	2	Citrate	2	4	LysoPC(14:0/0:0)	1	1	PC(34:2)	1	1
Acetylcarnitine	1	1	Citruline	3	3	LysoPC(15:0/0:0)	1	1	PC(36:2)	1	1
Acetylornithine	2	0	Coenzyme A	0	3	LysoPC(16:0/0:0)	0	2	PC(36:4)	1	1
Adenosine Monophosphate (AMP)	2	1	Creatine	4	3	LysoPC(18:0/0:0)	0	2	PC(38:6)	1	1
Alanine	6	5	Cytidine	1	1	LysoPC(18:1/0:0)	0	2	PE(34:1)	1	1
Alpha-Ketoglutarate	2	2	D-Glucose	1	1	LysoPC(18:2)	1	1	LysoPC(18:2)	1	1
Arachidonic Acid	4	4	Dimethyl Glycine	0	2	LysoPC(18:3/0:0)	0	2	LysoPC(18:3/0:0)	0	2
Arginine	4	5	D-Lactic Acid	0	2	LysoPC(20:0/0:0)	0	3	PE(38:2)	0	2
Asparagine	4	0	Docosahexaenoic Acid	0	2	LysoPC(20:1/0:0)	0	2	PE(38:4)	0	2
Aspartate	3	3	Docosapentaenoic Acid	0	2	LysoPC(20:2/0:0)	0	2	PE(38:6)	1	1
Butyrylcarnitine	2	0	Dodecanoylcarnitine	2	1	LysoPC(20:1/0:0)	0	2	PG(34:1)	1	1
C10:0 Carnitine	0	2	Ecosapentaenoic Acid	2	0	LysoPC(20:2/0:0)	0	2	PG(36:1)	1	1
C10:1 Carnitine	0	2	Eicosadienoic Acid	2	0	LysoPE(16:0/0:0)	0	2	PG(36:2)	1	1
C12:0 Carnitine	0	2	Formate	2	1	LysoPE(18:0/0:0)	0	2	PG(38:1)	1	1
C12:1 Carnitine	0	3	Fumarate	2	1	LysoPE(18:1)	0	2	PI(36:1)	1	1
C14:0 Carnitine	1	3	Glucose	2	1	LysoPE(20:0)	1	1	PI(38:4)	1	1
C14:1 Carnitine	0	4	Glutamate	2	6	LysoPE(20:3/0:0)	0	2	Pimelylcarnitine (C7-DC)	1	1
C14:2 Carnitine	0	3	Glutamine	7	2	LysoPI(20:4)	0	2	Proline	5	4
C16:0 Carnitine	0	4	Glutarylcarnitine (C5-DC)	1	1	LysoPS(18:0)	1	1	Propionylcarnitine	1	2
C16:1 Carnitine	0	3	Glycerin	1	1	Malate	3	1	Pyruvate	1	3
C16:2 Carnitine	0	4	Glycerol	1	1	Methionine	4	2	Serine	4	0
C18:0 Carnitine	1	2	Glycerophosphocholine	1	2	MG (16:0/0:0/0:0)	0	3	SM(d18:1/22:0)	0	2
C18:1 Carnitine	0	4	Glycine	7	1	Myo-Inositol	2	0	Sphingosine	2	0
C18:2 Carnitine	0	3	Hexanoylcarnitine	2	0	N-Acetylornithine	1	1	Sphingosine 1-Phosphate	3	0
C2:0 Carnitine	0	2	Homocysteic Acid	1	1	Oleic acid	2	2	Stearoylcarnitine	3	0
C4:0 Carnitine	1	1	Hypoxanthine	3	1	Phenylalanine	11	2	Succinate	6	2
C5:0 Carnitine	1	1	Inosine	3	1	Oleoylcarnitine	2	0	Taurine	4	3
C6:0 Carnitine	0	2	Isoleucine	8	3	Ornithine	3	2	Tetradecanoylcarnitine	1	1
C8:0 Carnitine	0	2	Isovalerylcarnitine	2	0	PA(36:2)	0	2	Tetradecenoylcarnitine	1	1
C8:0 Carnitine	0	3	Histidine	4	1	Nicotinamide	1	1	Stearic Acid	2	2
C8:1 Carnitine	0	2	Kynurenine	2	1	Palmitic Acid	3	3	Threonine	4	1
Uridine	2	2	Urea	2	0	Valine	9	2	Tryptophan	6	4
β-Glucose	2	0	Uric Acid	3	1	Xanthine	1	1	Tyrosine	6	3
Uracil	2	1									

Number of studies reported with up and down regulated levels of metabolites

Up	Down
0	0
1	1
2	2
3	3
4	4
5	5
6	6
7	
8	
9	
10	
11	

Fig. 4 Summary of significant metabolites affected by DIC identified in two or more studies. The size of the bar and the number in each box indicate the number of studies reported and whether the metabolite levels increased (up) or decreased (down)

identifiers used in HMDB ID, PubChem, ChEBI, METLIN, and KEGG. Out of the 462 metabolites, 231 were successfully matched to HMDB IDs, which were then mapped to KEGG human metabolic pathways for functional interpretation. Over-representation analysis (ORA) was conducted using the hypergeometric test to evaluate whether a particular metabolite set is represented more than expected by chance within the given list of 462 potential markers (Supplemental Table 2). Figure 5 summarizes metabolic pathways predicted to be affected using findings from all studies where arginine biosynthesis (FDR = 4.5E-07), citrate cycle (FDR = 3.1E-04) and alanine, aspartate, and glutamate metabolism (FDR = 7.4E-04) were highlighted as the top three metabolite sets enriched within the pre-defined metabolites from all studies. Similarly, we performed pathways enrichment analysis for each model studies (in vitro, rat, mouse, and human) (Supplemental Tables 3–6, Supplemental Fig. 1) and identified glyoxylate and dicarboxylate metabolism was the most affected pathway across the groups (Supplemental Fig. 2). In vitro studies uniquely exhibited alterations in cysteine and methionine metabolism as well as pyrimidine metabolism. Glutathione metabolism was exclusively impacted in mouse studies, while purine metabolism was distinct to human studies. In contrast, pyruvate metabolism, neomycin, kanamycin, and gentamicin biosynthesis, β-alanine metabolism, glycolysis/gluconeogenesis, glycerophospholipid metabolism, and lipoic acid metabolism were uniquely affected in rat studies. Five metabolic pathways were commonly affected across in vitro, rat, and mouse models, including pantothenate and CoA biosynthesis, arginine and proline metabolism, phenylalanine, tyrosine, and tryptophan biosynthesis, alanine, aspartate, and glutamate metabolism, and arginine biosynthesis. Four metabolic pathways—citrate cycle (TCA cycle), histidine metabolism, glycine, serine, and threonine metabolism, and butanoate metabolism—were commonly affected across rat, and mouse models. Additionally, valine, leucine, and isoleucine biosynthesis was the only pathway commonly affected across rat, mouse, and human models.

4 Discussion

DOX is a widely used chemotherapeutic agent, particularly effective in treating various types of cancers, including breast cancer (Devericks et al., 2022; Singal & Iliskovic, 1998). However, its clinical use is significantly limited due to its cardiotoxic effects (Devericks et al., 2022; Mohammed et al., 2021; Singal & Iliskovic, 1998). DIC involves oxidative stress, mitochondrial dysfunction, and apoptosis in cardiomyocytes (Aryal & Rao, 2016). This condition is a major concern in oncology, as it can lead to irreversible damage to the heart, manifesting as cardiomyopathy or heart failure. Metabolomics provides a powerful approach to understand the molecular underpinnings of DIC by profiling the metabolites altered in response to treatment. DOX accumulates in mitochondria of cardiomyocytes, hepatocytes, and blood cells, contributing to its immense dose-limiting toxic

Fig. 5 Over-Representation Analysis of metabolite findings from all studies using MetaboAnalyst

profile (Geng et al., 2021; Verheijen et al., 2018). The recommended cumulative total lifetime dose of DOX should not exceed 450–550 mg/m^2 body surface area, as the risk of congestive cardiac failure greatly increases beyond that dose (Rahman et al., 2007). Currently, the diagnosis is made based on clinical signs of HF, e.g., S3 gallop, jugular venous distention, nonspecific ST-T wave changes, low voltage QRS complexes, echocardiography to detect a change in LVEF, and elevation of serum Brain natriuretic peptide and troponin T levels (Chatterjee et al., 2010; Ky et al., 2014; Strigun et al., 2011). The development of these signs and symptoms indicates a point of no return and portends a poor prognosis (Mercuro et al., 2007). Several ongoing investigations aim to find highly sensitive and specific predictive biomarkers, so that early intervention may be started. Moreover, such biomarkers may point to potential new targets to detect the cardiotoxicity early.

Metabolomics, as an emerging field, is proving invaluable in identifying key metabolites involved in the pathogenesis of DIC, pinpointing specific biomarkers for early detection, treatment, and monitoring the effectiveness of interventions. In this systematic review, we identified four common metabolites (inosine, phenylalanine, arginine, and tryptophan) that were shared across all three study models (cell line, animal model, and human studies) (Andreadou et al., 2014; Finkelman et al., 2017; Niu et al., 2016; QuanJun et al., 2017; Schnackenberg et al., 2016; Tan et al., 2011; Thonusin et al., 2023a, 2024; Wang et al., 2020; Yi et al., 2018; Yuan et al., 2020; Zhang et al., 2021; Zhou et al., 2020).

Across all four study types (rat, mouse, cell line, and human), phenylalanine, arginine, and tryptophan were the most significantly perturbed metabolites. In a cell line study by Yi et al. (Yi et al., 2018), levels of these three metabolites were decreased due to DIC. Human studies, however, reported an increase in phenylalanine and tryptophan levels (Thonusin et al., 2024) and a decrease in arginine levels (Finkelman et al., 2017). In rat studies, tryptophan levels decreased in two studies (Thonusin et al., 2023a; Yuan et al., 2020) and increased in two others (Thonusin et al., 2023a; Zhou et al., 2020). Arginine levels increased in heart tissue but decreased in serum (Thonusin et al., 2023a). Phenylalanine levels were consistently increased in heart tissue and plasma samples across four studies (Andreadou et al., 2014; Niu et al., 2016; Thonusin et al., 2023a; Zhou et al., 2020). The SABRE study and the British Women's Health and Heart Study reported that higher phenylalanine levels are associated with increased cardiovascular risk (Würtz et al., 2015).

Pathway analyses from multiple studies have identified 231 perturbed metabolites with matching compound IDs across 28 studies, including pathways involved in arginine biosynthesis, TCA cycle, alanine, aspartate and glutamate metabolism, arginine and proline metabolism, glutathione metabolism, purine metabolism, and pyruvate metabolism. These pathways are primarily linked to mitochondrial energy metabolism, the TCA cycle, and β-oxidation of fatty acids, with their dysregulation leading to oxidative stress and impaired glutathione metabolism, contributing to DOX induced toxicity (Li et al., 2019; Rushing et al., 2023; Zheng et al., 2019). Figure 5 and Supplemental Table 2 summarize the widespread early effects of DOX treatment on these metabolic pathways.

The arginine biosynthesis pathway is essential for cardiovascular health, playing a role in NO production, energy metabolism, and the urea cycle (Finkelman et al., 2017; Li et al., 2019). DIC significantly disrupts this pathway, affecting key metabolites such as glutamic acid, L-arginine, citrulline, and ornithine. N2-acetylornithine is vital for the conversion processes leading to citrulline and arginine synthesis, while L-aspartic acid participates in the urea cycle and amino acid biosynthesis, helping maintain nitrogen balance (Finkelman et al., 2017). Under stress conditions like cardiotoxicity, metabolic disruptions involving these metabolites occur. In this review, we found a decrease in L-aspartic acid levels in rat serum samples (QuanJun et al., 2017) and cell line studies (Yi et al., 2018), while levels increased in rat serum and heart tissue samples (Andreadou et al., 2014; Thonusin et al., 2023a). Oxoglutaric acid, a key component of the TCA cycle and amino acid metabolism, influences oxidative stress pathways and energy production, both critical for protecting cardiac function under toxic stress (An et al., 2021; Chen et al., 2018). We observed that alpha-ketoglutarate levels in heart tissue and serum samples increased in a rat study due to DOX treatment (Thonusin et al., 2023a), whereas other rat and mouse studies reported a decrease in alpha-ketoglutaric acid in plasma (Yuan et al., 2020) and serum samples (Xue et al., 2023). Similarly, an increase in 2-oxoglutarate was found in serum samples in mice studies (QuanJun et al., 2017). Fumaric acid, another TCA cycle intermediate, plays a vital role in energy production, and its dysregulation can indicate metabolic distress in cardiac cells, particularly under oxidative stress or hypoxic conditions common in HF (Ashrafian et al., 2012; Pravenec et al., 2014). Fumaric acid was found to increase (Andreadou et al., 2014) and decrease (Niu et al., 2016) after DOX treatment in rat heart tissue. Additionally, proline and hydroxyproline, crucial for collagen synthesis (Levick et al., 2019), are disrupted in DOX treatment, contributing to structural damage and fibrosis (Fenwick et al., 2019). Two studies reported a decrease in proline levels in rat (Alhazzani et al., 2021) and mouse (Geng et al., 2021) serum samples, while one study observed an increase in proline levels in rat serum samples (Xue et al., 2023). Impairment of the

creatine cycle further exacerbates ATP deficits, weakening cardiac function.

Glutamine levels were reported to increase in both heart tissue and plasma (Andreadou et al., 2009, 2014; Niu et al., 2016; Schnackenberg et al., 2016; Tan et al., 2011; Thonusin et al., 2023a, 2024), However, a decrease in glutamine levels was observed in heart tissue (Thonusin et al., 2023a) and serum (Yuan et al., 2020) due to DIC in rat studies. Glutamine metabolism is a key aspect of metabolic reprogramming, closely linked to amino acid transporters. Glutamine serves as a substrate in the de novo purine biosynthesis pathway (Mayers et al., 2016). While glutamine is non-essential for normal cells, highly proliferative cancer cells rely on it as an essential substrate for energy production and the synthesis of nucleotides, lipids, and proteins. In breast cancer, amino acid transporters SLC1A5 and SLC6A14 are upregulated to transport glutamine (Kim et al., 2013; Van Geldermalsen et al., 2016), significantly impacting tumor biology. In lung and breast cancers, glutamine transport plays a crucial role in influencing cellular metabolism, growth, and survival via mTOR signaling (Hassanein et al., 2013; Moses & Neckers, 2015). Additionally, mTOR can modify amino acid substrates such as glycine and aspartate in de novo purine biosynthesis within certain tumors (Allen et al., 2016; Locasale, 2013).

The citrate cycle (TCA cycle) is critical for energy production, and its disruption is closely associated with cardiotoxicity, particularly in response to treatments like DOX. Key metabolites such as oxoglutaric acid, succinic acid, malic acid, and citric acid play essential roles in ATP production. Thiamine pyrophosphate, a cofactor in the TCA cycle, is crucial for decarboxylation reactions, while 3-carboxy-1-hydroxypropylthiamine diphosphate is an intermediate in thiamine-dependent reactions. In this systematic review, we observed that thiamine diphosphate levels decreased in rat heart tissue after DOX treatment (Chen et al., 2015). Additionally, in cell lines and mouse studies, the levels of 3-carboxy-1-hydroxypropylthiamine diphosphate were found to be reduced (Wen et al., 2020b, 2020c). However, the level of succinic acid was found to increase in serum, plasma, and heart tissue (Andreadou et al., 2009, 2014; Schnackenberg et al., 2016; Tan et al., 2011; Thonusin et al., 2023a, 2023b), with only one study reporting a reduced level in rat serum samples (Niu et al., 2016). Succinic acid signals mitochondrial dysfunction when dysregulated, a hallmark of DIC. Malic acid facilitates energy conversion to ATP, and citric acid disruptions can impair the entire cycle, reducing energy production and increasing oxidative stress. In this review, the level of malic acid was found to increase in heart tissue samples of rats and mice (Tan et al., 2011; Thonusin et al., 2023a), and in plasma samples of humans (Thonusin et al., 2024). Impaired pyruvate to acetyl-CoA conversion results in lactate accumulation, while fumarate is necessary for oxaloacetate regeneration. Pyruvic acid levels were found to decrease in rat serum samples (Niu et al., 2016), and cell line studies (Chaudhari et al., 2017). Phosphoenolpyruvic acid, involved in glycolysis and gluconeogenesis, maintains energy balance, and disruptions in its metabolism can worsen cardiac energy deficits. Monitoring these intermediates provides insight into metabolic dysfunction and identifies therapeutic targets to mitigate cardiotoxicity.

In DIC, the alanine, aspartate, and glutamate metabolism pathways are also disrupted, impairing energy production and amino acid balance. Key metabolites such as L-aspartic acid, L-alanine, glutamic acid, and glutamine play critical roles in energy metabolism and response to oxidative stress (Antonarelli et al., 2021; Watanabe et al., 2021). L-aspartic acid, essential for the urea cycle and nucleotide synthesis, is disrupted in cardiotoxicity, affecting energy metabolism and protein synthesis (Sivakumar et al., 2008, 2011). L-alanine, crucial for the glucose-alanine cycle, regulates glucose levels and energy production, while impaired metabolism exacerbates energy deficits in cardiac cells (Fernandez-Caggiano et al., 2020; Lee et al., 2020). Glutamic acid, central to amino acid metabolism and a precursor to glutamine, maintains nitrogen balance and supports energy production through the TCA cycle (Yoo et al., 2020). Its disruption increases oxidative stress, worsening cardiotoxic effects (Watanabe et al., 2021). Citric acid, a key component of the TCA cycle, is essential for ATP production, and its disruption impairs energy metabolism in cardiotoxicity (Doenst et al., 2013). Pyruvic acid links glycolysis to the TCA cycle, and its impaired metabolism reduces energy production, increasing lactate and worsening heart dysfunction (Lopaschuk et al., 2021). Succinic acid, vital for ATP generation, and oxoglutaric acid, crucial for amino acid metabolism, also face dysregulation, leading to oxidative stress and impaired energy production (Chouchani et al., 2014; Zhang et al., 2020). These disruptions may contribute to mitochondrial dysfunction, reduced ATP production, and cardiac damage, highlighting them as potential therapeutic targets for cardiotoxicity prevention.

Glyoxylate and dicarboxylate metabolism plays a key role in DIC, intersecting with energy production and oxidative stress pathways. A nested case–control plasma metabolomics study in coronary artery disease patients (Lv et al., 2024) identified it, along with the TCA cycle, as one of the most affected pathways. Perturbations in key metabolites (citric acid and malic acid) indicate mitochondrial dysfunction, oxidative stress, and energy dysregulation, emphasizing their role in cardiotoxicity and potential cardioprotective targets (Geng et al., 2024).

The myocardium relies mainly on fatty acid oxidation followed by glycolysis as an energy source for its high

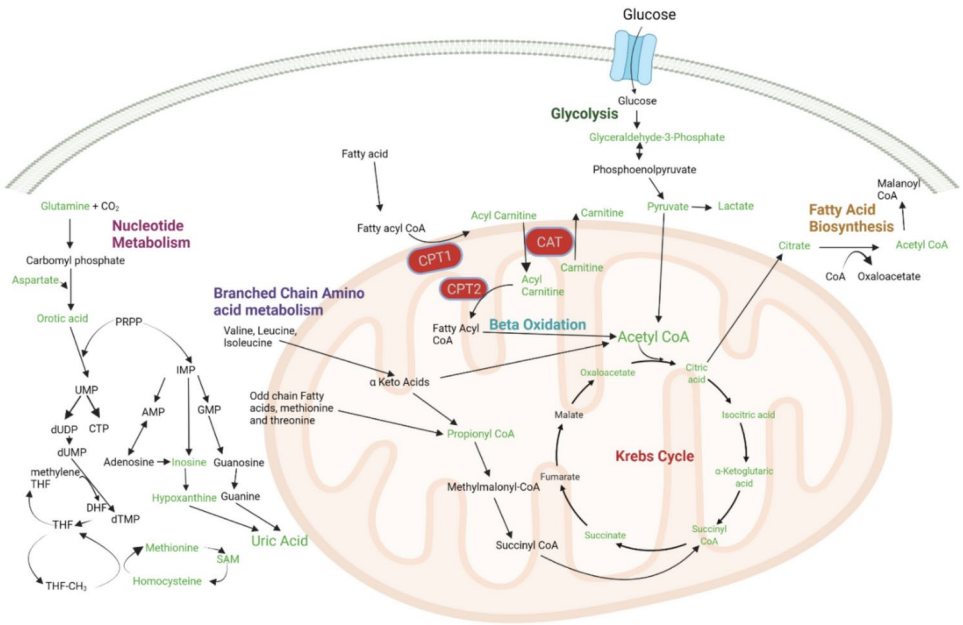

Fig. 6 Perturbed metabolic pathways and metabolites (Green) in DOX-induced cardiotoxicity. *PRPP* Phosphoribosyl pyrophosphate, *UMP* Uridine monophosphate, *IMP* Inosine monophosphate, *AMP* Adenosine Monophosphate, *GMP* Guanosine monophosphate, *dTMP* Deoxythymidine monophosphate, *THF* Tetrahydrofolate, *DHF* Dihydrofolate, *CoA* Coenzyme A, *CPT 1* Carnitine palmitoyltranferase 1, *CPT2* Carnitine palmitoyltranferase 2, *CAT* Carnitine/acylcarnitine translocase. BioRender was used to create the figure (Color figure online)

metabolic requirements. However, depending on substrate concentration, lactate, ketone bodies, amino acids and, acetate can be used as alternative energy sources (Kodde et al., 2007). Animal and cell culture studies have repeatedly shown altered levels of acylcarnitine, glycerolipids, cholesterol, palmitic acid, and stearic acid after DOX treatment (Table 1) (Geng et al., 2021; Thonusin et al., 2023a). An upward trend in stearic acid with a reduction in acetone/acetoacetate suggests inhibition of β-oxidation of fatty acids (Andreadou et al., 2014; Tan et al., 2011; Wang et al., 2020; Zhang et al., 2021). Proteomics has shown dose-dependent downregulation of mitochondrial carnitine/acylcarnitine carrier; this prevents entry of long-chain acetyl-CoA into the mitochondria, reducing the β-oxidation of fatty acids and mitochondrial energy production (Niu et al., 2016; Schnackenberg et al., 2016).

Identifying metabolites involved in energy metabolism is at the core of understanding DIC (Fig. 6). To this end, studies have identified reduced levels of α-ketoglutarate, citrate, branched-chain amino acids (valine and isoleucine) together with elevated succinate, malate, acetate levels, among others (Supplemental Table 1) (Andreadou et al., 2009; Chaudhari et al., 2017; Tan et al., 2011). Hypotheses involving reduced activities of succinate dehydrogenase and malate dehydrogenase have emerged. However, data supporting a role for oxidative stress are still strong. DOX is reduced by mitochondrial complex I (NADH: ubiquinone oxidoreductase), which is abundant in the mitochondria of cardiomyocytes. This forms a semiquinone that leads to the generation of reactive oxygen species, with depleted levels of glutathione exacerbating cardiotoxicity. DOX also reacts with transitional metals such as iron to form similar free radicals. This damages the phospholipid bilayers, membrane proteins, and the membrane permeability (Carvalho et al., 2014; QuanJun et al., 2017; Verheijen et al., 2018).

Biomarker discovery is often hampered by low translational success rates. We are aware that the metabolomics approaches reviewed in this study contained in vitro studies from various origins (rat embryonic cardiomyocytes, mouse cardiomyocytes, human cardiomyocytes in the cell culture system) and different strains of animals (Sprague–Dawley rats, Wistar rats, B6C3F1 mice, ICR mice, C57BL/6 and BALB/c mice), all providing valuable preclinical information between basic research and clinical practice. Here, we want to highlight that of all the studies reviewed examining biomarkers of chemotherapy-induced cardiotoxicity, only one study used tumor bearing animals although it was not a breast cancer model (QuanJun et al., 2017). Cancer is a systemic disease, characterized by an altered metabolism with increased uptake and utilization of glucose to achieve increased energy requirements and involving not just the tumor, but a systematic dysfunction in the immune surveillance and microenvironment that allows cancer progression (Egeblad et al., 2010; McAllister & Weinberg, 2010).

This review has some strengths. First, it systematically compiles and evaluates existing literature on the metabolomic assessment of DIC, providing a comprehensive overview of available data from different model systems. Second, the integration of data from in vitro, animal, and human studies provides a translational perspective, aiding in understanding the mechanistic underpinnings of DIC and potential clinical applications. Third, pathway enrichment analysis provides insights into metabolic alterations associated with DIC, supporting future biomarker discovery

and therapeutic target identification. Fourth, the use of systematic search criteria and structured eligibility assessment enhances the reproducibility and reliability of findings.

The review was limited to the variability in study designs, sample sizes, and analytical methodologies among the included studies, which may introduce bias and reduce comparability. The majority of included studies focused on preclinical models, limiting the direct clinical applicability of findings. Differences in metabolomic platforms and analytical approaches across studies may result in inconsistencies in reported metabolites and pathway associations. The relatively small number of human studies included in the analysis limits the generalizability of findings to broader patient populations. A significant challenge in metabolomics is ensuring the accurate identification of differential metabolites. Biological samples are inherently complex, containing thousands of metabolites. Advanced techniques such as mass spectrometry (MS) and nuclear magnetic resonance (NMR) provide valuable data; however, accurately identifying metabolites remains difficult due to signal overlap and high variability. Many laboratories rely on commercial product libraries, which may not always be comprehensive or of high quality. Ideally, metabolomics studies should use authentic standards—known compounds with well-characterized structures and properties—to enhance metabolite identification reliability. However, acquiring authentic standards for all metabolites in a sample is often impractical due to cost and availability constraints. As a result, researchers frequently depend on commercial libraries, which can introduce systematic biases or inaccuracies. Properly constructed and maintained in-house libraries could mitigate these issues, but establishing such resources demands significant time, expertise, and financial investment, making them infeasible for many laboratories. Metabolite identification is further complicated by the presence of structural isomers, which are challenging to differentiate without well-characterized standards. Misidentification can lead to incorrect conclusions in biomarker discovery. Additionally, statistical analysis in metabolomics presents another major challenge. Given the large number of variables being tested simultaneously, researchers must use appropriate statistical methods to control for false discoveries and address the multiple testing problem. However, many metabolomics studies still employ simplistic or inadequate statistical approaches, leading to inflated false-positive rates or the omission of true biological signals. Inconsistent application of significance thresholds, such as p-values or false discovery rates, further exacerbates these issues.

To address the limitations of current studies, future research should incorporate several key strategies by incorporating multi-omics approaches, expanding clinical validation efforts, and ensuring standardization in metabolomics methodologies to improve the translational impact of the findings. To improve reproducibility and reliability, researchers should adopt rigorous statistical models and validation strategies, including cross-validation and bootstrapping. Implementing standardized reporting practices, such as those outlined by the Metabolomics Standards Initiative (MSI), can enhance study transparency and comparability. A checklist or reporting guideline, such as Clear documentation of sample preparation protocols, analytical methods, instrument settings, metabolite identification procedures, and statistical analyses will strengthen the field, ultimately leading to more robust biomarker discovery and scientific outcomes.

5 Conclusions

In conclusion, while efforts to identify metabolite biomarkers for DIC have highlighted important metabolic pathways, a definitive set of biomarkers remains elusive. Future research should prioritize untargeted metabolomics in DOX-treated rat models and clinical patients, with standardized treatment protocols to improve predictive biomarker identification. Comparing data from tumor bearing models and cancer patients will help address species-specific differences and enhance translational potential of findings. Additionally, using female tumor-bearing animal models may provide more relevant comparisons to breast cancer patients. Therapeutic interventions must ensure that chemotherapy's anti-tumor effects are preserved while protecting the heart. Understanding the metabolic disturbances induced by DOX, such as those affecting arginine and proline metabolism and the TCA cycle, have the potential of the early identification of patients at risk for DIC and can guide strategies to mitigate cardiotoxicity by restoring metabolic balance and reducing oxidative stress.

Supplementary Information The online version contains supplementary material available at https://doi.org/10.1007/s11306-025-02258-8.

Acknowledgements The authors thank Sheila Louise Thomas and Lindsay Blake for their help in compiling the literatures.

Author contributions AS, M. Bakhtyar, SM, and PCH conceived and designed the research. AS, M. Bakhtyar conducted the literature review and wrote the first draft of the manuscript. AS, M. Bakhtyar, PCH, and SRJ analyzed the data. AS, M. Boerma, RSL, and PCH critically appraised the manuscript. All authors read and approved the manuscript.

Funding This study was funded by the National Institute of General Medical Sciences (P20 GM109005). The authors declare no conflict of interest.

Data availability No datasets were generated or analysed during the current study.

Declarations

Conflict of interest The authors declare no competing interests.

Ethical approval This article does not contain any studies with human participants or animals performed by any of the authors.

References

Alhazzani, K., Alotaibi, M. R., Alotaibi, F. N., Aljerian, K., As Sobeai, H. M., Alhoshani, A. R., Alanazi, A. Z., Alanazi, W. A., & Alswayyed, M. (2021). Protective effect of valsartan against doxorubicin-induced cardiotoxicity: Histopathology and metabolomics in vivo study. *Journal of Biochemical and Molecular Toxicology*. https://doi.org/10.1002/jbt.22842

Allemani, C., Matsuda, T., Di Carlo, V., Harewood, R., Matz, M., Nikšić, M., Bonaventure, A., Valkov, M., Johnson, C. J., Estève, J., Ogunbiyi, O. J., & Azevedo e Silva Chen Eser Engholm Stiller Monnereau Woods Visser Lewis, G. W. Q. S. G. C. A. A. R. R. O. C. (2018). Global surveillance of trends in cancer survival 2000–14 (CONCORD-3): analysis of individual records for 37 513 025 patients diagnosed with one of 18 cancers from 322 population-based registries in 71 countries. *The Lancet,391*(10125), 1023–1075. https://doi.org/10.1016/S0140-6736(17)33326-3

Allen, E. L., Ulanet, D. B., Pirman, D., Mahoney, C. E., Coco, J., Si, Y., Chen, Y., Huang, L., Ren, J., & Choe, S. (2016). Differential aspartate usage identifies a subset of cancer cells particularly dependent on OGDH. *Cell Reports,17*(3), 876–890.

An, D., Zeng, Q., Zhang, P., Ma, Z., Zhang, H., Liu, Z., Li, J., Ren, H., & Xu, D. (2021). Alpha-ketoglutarate ameliorates pressure overload-induced chronic cardiac dysfunction in mice. *Redox Biology,46*, Article 102088.

Anderson, R. A., Clatot, F., Demeestere, I., Lambertini, M., Morgan, A., Nelson, S. M., Peccatori, F., & Cameron, D. (2021). Cancer survivorship: Reproductive health outcomes should be included in standard toxicity assessments. *European Journal of Cancer,144*, 310–316. https://doi.org/10.1016/j.ejca.2020.11.032

Andreadou, I., Mikros, E., Ioannidis, K., Sigala, F., Naka, K., Kostidis, S., Farmakis, D., Tenta, R., Kavantzas, N., Bibli, S.-I., Gikas, E., Skaltsounis, L., Kremastinos, D. T., & Iliodromitis, E. K. (2014). Oleuropein prevents doxorubicin-induced cardiomyopathy interfering with signaling molecules and cardiomyocyte metabolism. *Journal of Molecular and Cellular Cardiology,69*, 4–16. https://doi.org/10.1016/j.yjmcc.2014.01.007

Andreadou, I., Papaefthimiou, M., Zira, A., Constantinou, M., Sigala, F., Skaltsounis, A. L., Tsantili-Kakoulidou, A., Iliodromitis, E. K., Kremastinos, D. T., & Mikros, E. (2009). Metabonomic identification of novel biomarkers in doxorubicin cardiotoxicity and protective effect of the natural antioxidant oleuropein. *NMR in Biomedicine,22*(6), 585–592. https://doi.org/10.1002/nbm.1370

Antonarelli, G., Corti, C., Tarantino, P., Ascione, L., Cortes, J., Romero, P., Mittendorf, E., Disis, M., & Curigliano, G. (2021). Therapeutic cancer vaccines revamping: Technology advancements and pitfalls. *Annals of Oncology,32*(12), 1537–1551.

Aryal, B., & Rao, V. A. (2016). Deficiency in cardiolipin reduces doxorubicin-induced oxidative stress and mitochondrial damage in human B-lymphocytes. *PLoS ONE,11*(7), Article e0158376.

Ashrafian, H., Czibik, G., Bellahcene, M., Aksentijević, D., Smith, A. C., Mitchell, S. J., Dodd, M. S., Kirwan, J., Byrne, J. J., Ludwig, C., Isackson, H., Yavari, A., Støttrup, N. B., Contractor, H., Cahill, T. J., Sahgal, N., Ball, D. R., Birkler, R. I., Hargreaves, I., & Watkins, H. (2012). Fumarate is cardioprotective via activation of the Nrf2 antioxidant pathway. *Cell Metabolism,15*(3), 361–371. https://doi.org/10.1016/j.cmet.2012.01.017

Asnani, A., Shi, X., Farrell, L., Lall, R., Sebag, I. A., Plana, J. C., Gerszten, R. E., & Scherrer-Crosbie, M. (2020). Changes in citric acid cycle and nucleoside metabolism are associated with anthracycline cardiotoxicity in patients with breast cancer. *Journal of Cardiovascular Translational Research,13*(3), 349–356. https://doi.org/10.1007/s12265-019-09897-y

Bhat, O. M., Mir, R. A., Nehvi, I. B., Wani, N. A., Dar, A. H., & Zargar, M. A. (2024). Emerging role of sphingolipids and extracellular vesicles in development and therapeutics of cardiovascular diseases. *IJC Heart & Vasculature,53*, 101469. https://doi.org/10.1016/j.ijcha.2024.101469

Blais, E. M., Rawls, K. D., Dougherty, B. V., Li, Z. I., Kolling, G. L., Ye, P., Wallqvist, A., & Papin, J. A. (2017). Reconciled rat and human metabolic networks for comparative toxicogenomics and biomarker predictions. *Nature Communications,8*, 14250. https://doi.org/10.1038/ncomms14250

Borodzicz-Jażdżyk, S., Jażdżyk, P., Łysik, W., Cudnoch-Jędrzejewska, A., & Czarzasta, K. (2022). Sphingolipid metabolism and signaling in cardiovascular diseases. *Frontiers in Cardiovascular Medicine,9*, Article 915961. https://doi.org/10.3389/fcvm.2022.915961

Bryda, E. C. (2013). The mighty mouse: The impact of rodents on advances in biomedical research. *Missouri Medicine,110*, 4.

Camilli, M., Cipolla, C. M., Dent, S., Minotti, G., & Cardinale, D. M. (2024). Anthracycline cardiotoxicity in adult cancer patients. *JACC: Cardiooncology,6*(5), 655–677. https://doi.org/10.1016/j.jaccao.2024.07.016

Cardinale, D., Colombo, A., Bacchiani, G., Tedeschi, I., Meroni, C. A., Veglia, F., Civelli, M., Lamantia, G., Colombo, N., Curigliano, G., Fiorentini, C., & Cipolla, C. M. (2015). Early detection of anthracycline cardiotoxicity and improvement with heart failure therapy. *Circulation,131*(22), 1981–1988. https://doi.org/10.1161/CIRCULATIONAHA.114.013777

Carvalho, F. S., Burgeiro, A., Garcia, R., Moreno, A. J., Carvalho, R. A., & Oliveira, P. J. (2014). Doxorubicin-induced cardiotoxicity: From bioenergetic failure and cell death to cardiomyopathy. *Medicinal Research Reviews,34*(1), 106–135. https://doi.org/10.1002/med.21280

Chatterjee, K., Zhang, J., Honbo, N., & Karliner, J. S. (2010). Doxorubicin cardiomyopathy. *Cardiology,115*(2), 155–162. https://doi.org/10.1159/000265166

Chaudhari, U., Ellis, J. K., Wagh, V., Nemade, H., Hescheler, J., Keun, H. C., & Sachinidis, A. (2017). Metabolite signatures of doxorubicin induced toxicity in human induced pluripotent stem cell-derived cardiomyocytes. *Amino Acids,49*(12), 1955–1963. https://doi.org/10.1007/s00726-017-2419-0

Chen, P., Hou, L., Luo, Y., Chen, L., Li, S., Lei, X., Huang, J., & Wu, D. (2018). Effect of diabetes on the assessment role of 2-oxoglutarate

to the severity of chronic heart failure. *Experimental and Clinical Endocrinology & Diabetes,126*(08), 478–486.

Chen, Y., Tang, Y., Zhang, Y. C., Huang, X. H., Xie, Y. Q., & Xiang, Y. (2015). A metabolomic study of rats with doxorubicin-induced cardiomyopathy and Shengmai injection treatment. *PLoS ONE,10*(5), Article e0125209. https://doi.org/10.1371/journal.pone.0125209

Chouchani, E. T., Pell, V. R., Gaude, E., Aksentijević, D., Sundier, S. Y., Robb, E. L., Logan, A., Nadtochiy, S. M., Ord, E. N. J., Smith, A. C., Eyassu, F., Shirley, R., Hu, C. H., Dare, A. J., James, A. M., Rogatti, S., Hartley, R. C., Eaton, S., Costa, A. S. H., & Murphy, M. P. (2014). Ischaemic accumulation of succinate controls reperfusion injury through mitochondrial ROS. *Nature,515*(7527), 431–435. https://doi.org/10.1038/nature13909

Clish, C. B. (2015). Metabolomics: An emerging but powerful tool for precision medicine. *Cold Spring Harb Mol Case Stud,1*(1), Article a000588. https://doi.org/10.1101/mcs.a000588

Cocco, D., Ferro, E. G., Ricci, S., Deidda, M., Noto, A., Madeddu, C., Atzori, F., Scartozzi, M., Mercuro, G., Cadeddu Dessalvi, C., University of Cagliari, I. (2020). Defining the metabolomic profile associated with early cardiotoxicity in patients with breast cancer treated with anthracyclines. *European Heart Journal*. https://doi.org/10.1093/ehjci/ehaa946.3289

Deidda, M., Mercurio, V., Cuomo, A., Noto, A., Mercuro, G., & Cadeddu Dessalvi, C. (2019). Metabolomic perspectives in antiblastic cardiotoxicity and cardioprotection. *International Journal of Molecular Sciences*. https://doi.org/10.3390/ijms20194928

Devericks, E. N., Carson, M. S., McCullough, L. E., Coleman, M. F., & Hursting, S. D. (2022). The obesity-breast cancer link: A multidisciplinary perspective. *Cancer and Metastasis Reviews,41*(3), 607–625. https://doi.org/10.1007/s10555-022-10043-5

Ding, X., Zhang, Y., Pan, P., Long, C., Zhang, X., Zhuo, L., Zhou, Q., Liao, W., & Tan, G. (2023). Multiple mitochondria-targeted components screened from Sini decoction improved cardiac energetics and mitochondrial dysfunction to attenuate doxorubicin-induced cardiomyopathy. *Theranostics,13*(2), 510–530. https://doi.org/10.7150/thno.80066

Doenst, T., Nguyen, T. D., & Abel, E. D. (2013). Cardiac metabolism in heart failure: Implications beyond ATP production. *Circulation Research,113*(6), 709–724. https://doi.org/10.1161/circresaha.113.300376

Egeblad, M., Nakasone, E. S., & Werb, Z. (2010). Tumors as organs: Complex tissues that interface with the entire organism. *Developmental Cell,18*(6), 884–901. https://doi.org/10.1016/j.devcel.2010.05.012

Feijen, E. A. M., Leisenring, W. M., Stratton, K. L., Ness, K. K., van der Pal, H. J. H., van Dalen, E. C., Armstrong, G. T., Aune, G. J., Green, D. M., Hudson, M. M., Loonen, J., Oeffinger, K. C., Robison, L. L., Yasui, Y., Kremer, L. C. M., & Chow, E. J. (2019). Derivation of anthracycline and anthraquinone equivalence ratios to doxorubicin for late-onset cardiotoxicity. *JAMA Oncology,5*(6), 864–871. https://doi.org/10.1001/jamaoncol.2018.6634

Fenwick, A. J., Awinda, P. O., Yarbrough-Jones, J. A., Eldridge, J. A., Rodgers, B. D., & Tanner, B. C. W. (2019). Demembranated skeletal and cardiac fibers produce less force with altered cross-bridge kinetics in a mouse model for limb-girdle muscular dystrophy 2i. *American Journal of Physiology-Cell Physiology,317*(2), C226–C234. https://doi.org/10.1152/ajpcell.00524.2018

Fernandez-Caggiano, M., Kamynina, A., Francois, A. A., Prysyazhna, O., Eykyn, T. R., Krasemann, S., Crespo-Leiro, M. G., Vieites, M. G., Bianchi, K., & Morales, V. (2020). Mitochondrial pyruvate carrier abundance mediates pathological cardiac hypertrophy. *Nature Metabolism,2*(11), 1223–1231.

Finkelman, B. S., Putt, M., Wang, T., Wang, L., Narayan, H., Domchek, S., DeMichele, A., Fox, K., Matro, J., Shah, P., Clark, A., Bradbury, A., Narayan, V., Carver, J. R., Tang, W. H. W., & Ky, B. (2017). Arginine-nitric oxide metabolites and cardiac dysfunction in patients with breast cancer. *Journal of the American College of Cardiology,70*(2), 152–162. https://doi.org/10.1016/j.jacc.2017.05.019

Foran, D., Antoniades, C., & Akoumianakis, I. (2024). Emerging roles for sphingolipids in cardiometabolic disease: A rational therapeutic target? *Nutrients,16*(19), 3296.

Gawlik, M., Zimodro, J. M., Gąsecka, A., Filipiak, K. J., & Szmit, S. (2023). Cardiac arrhythmias in oncological patients-epidemiology, risk factors, and management within the context of the new ESC 2022 guidelines. *Current Oncology Reports,25*(10), 1107–1115. https://doi.org/10.1007/s11912-023-01445-x

Geng, C., Cui, C., Wang, C., Lu, S., Zhang, M., Chen, D., & Jiang, P. (2021). Systematic evaluations of doxorubicin-induced toxicity in rats based on metabolomics. *ACS Omega,6*(1), 358–366. https://doi.org/10.1021/acsomega.0c04677

Geng, C., Liang, B., Kong, Z., Feng, L., Wang, J., Si, Q., & Jiang, P. (2024). Metabolomic profiling reveals biomarkers in coronary heart disease comorbidity. *Journal of Diabetes Research,2024*, 8559677. https://doi.org/10.1155/jdr/8559677

Gibbs, R. A., Weinstock, G. M., Metzker, M. L., Muzny, D. M., Sodergren, E. J., Scherer, S., Scott, G., Steffen, D., Worley, K. C., Burch, P. E., Okwuonu, G., Hines, S., Lewis, L., DeRamo, C., Delgado, O., Dugan-Rocha, S., Miner, G., Morgan, M., Hawes, A., Rat Genome Sequencing Project, C. (2004). Genome sequence of the Brown Norway rat yields insights into mammalian evolution. *Nature,428*(6982), 493–521. https://doi.org/10.1038/nature02426

Gottdiener, J. S., Bednarz, J., Devereux, R., Gardin, J., Klein, A., Manning, W. J., Morehead, A., Kitzman, D., Oh, J., Quinones, M., Schiller, N. B., Stein, J. H., Weissman, N. J., American Society of, E. (2004). American Society of Echocardiography recommendations for use of echocardiography in clinical trials. *Journal of the American Society of Echocardiography,17*(10), 1086–1119. https://doi.org/10.1016/j.echo.2004.07.013

Hassanein, M., Hoeksema, M. D., Shiota, M., Qian, J., Harris, B. K., Chen, H., Clark, J. E., Alborn, W. E., Eisenberg, R., & Massion, P. P. (2013). SLC1A5 mediates glutamine transport required for lung cancer cell growth and survival. *Clinical Cancer Research,19*(3), 560–570.

Hausner, E. A., Hicks, K. A., Leighton, J. K., Szarfman, A., Thompson, A. M., & Harlow, P. (2013). Qualification of cardiac troponins for nonclinical use: A regulatory perspective. *Regulatory Toxicology and Pharmacology,67*(1), 108–114. https://doi.org/10.1016/j.yrtph.2013.07.006

Heemelaar, J. C., Speetjens, F. M., Al Jaff, A. A. M., Evenhuis, R. E., Polomski, E. A. S., Mertens, B. J. A., Jukema, J. W., Gelderblom, H., van de Sande, M. A. J., & Antoni, M. L. (2023). Impact of age at diagnosis on cardiotoxicity in high-grade osteosarcoma and ewing sarcoma patients. *JACC CardioOncol,5*(1), 117–127. https://doi.org/10.1016/j.jaccao.2022.11.016

Herman, E. H., Lipshultz, S. E., Rifai, N., Zhang, J., Papoian, T., Yu, Z. X., Takeda, K., & Ferrans, V. J. (1998). Use of cardiac troponin T levels as an indicator of doxorubicin-induced cardiotoxicity. *Cancer Research,58*(2), 195–197.

Khan, M. A., Singh, D., Arif, A., Sodhi, K. K., Singh, D. K., Islam, S. N., Ahmad, A., Akhtar, K., & Siddique, H. R. (2022). Protective effect of green synthesized Selenium Nanoparticles against doxorubicin induced multiple adverse effects in Swiss albino mice. *Life Sciences,305*, Article 120792. https://doi.org/10.1016/j.lfs.2022.120792

Kim, S., Kim, D. H., Jung, W.-H., & Koo, J. S. (2013). Expression of glutamine metabolism-related proteins according to molecular subtype of breast cancer. *Endocrine-Related Cancer,20*(3), 339–348.

Kodde, I. F., van der Stok, J., Smolenski, R. T., & de Jong, J. W. (2007). Metabolic and genetic regulation of cardiac energy substrate

preference. *Comparative Biochemistry and Physiology Part a: Molecular & Integrative Physiology,146*(1), 26–39. https://doi.org/10.1016/j.cbpa.2006.09.014

Ky, B., Putt, M., Sawaya, H., French, B., Januzzi, J. L., Jr., Sebag, I. A., Plana, J. C., Cohen, V., Banchs, J., Carver, J. R., Wiegers, S. E., Martin, R. P., Picard, M. H., Gerszten, R. E., Halpern, E. F., Passeri, J., Kuter, I., & Scherrer-Crosbie, M. (2014). Early increases in multiple biomarkers predict subsequent cardiotoxicity in patients with breast cancer treated with doxorubicin, taxanes, and trastuzumab. *Journal of the American College of Cardiology,63*(8), 809–816. https://doi.org/10.1016/j.jacc.2013.10.061

Lee, S.-H., Hadipour-Lakmehsari, S., Kim, D. H., Di Paola, M., Kuzmanov, U., Shah, S., Lee, J.J.-H., Kislinger, T., Sharma, P., & Oudit, G. Y. (2020). Bioinformatic analysis of membrane and associated proteins in murine cardiomyocytes and human myocardium. *Scientific Data,7*(1), 425.

Levick, S. P., Soto-Pantoja, D. R., Bi, J., Hundley, W. G., Widiapradja, A., Manteufel, E. J., Bradshaw, T. W., & Meléndez, G. C. (2019). Doxorubicin-induced myocardial fibrosis involves the neurokinin-1 receptor and direct effects on cardiac fibroblasts. *Heart Lung Circulation,28*(10), 1598–1605. https://doi.org/10.1016/j.hlc.2018.08.003

Li, X., Gu, J., Zhang, Y., Feng, S., Huang, X., Jiang, Y., Xia, Y., Liu, Y., & Yang, X. (2019). l-arginine alleviates doxorubicin-induced endothelium-dependent dysfunction by promoting nitric oxide generation and inhibiting apoptosis. *Toxicology,423*, 105–111. https://doi.org/10.1016/j.tox.2019.05.016

Locasale, J. W. (2013). Serine, glycine and one-carbon units: Cancer metabolism in full circle. *Nature Reviews Cancer,13*(8), 572–583.

Lopaschuk, G. D., Karwi, Q. G., Tian, R., Wende, A. R., & Abel, E. D. (2021). Cardiac energy metabolism in heart failure. *Circulation Research,128*(10), 1487–1513. https://doi.org/10.1161/circresaha.121.318241

Lv, J., Pan, C., Cai, Y., Han, X., Wang, C., Ma, J., Pang, J., Xu, F., Wu, S., Kou, T., Ren, F., Zhu, Z. J., Zhang, T., Wang, J., & Chen, Y. (2024). Plasma metabolomics reveals the shared and distinct metabolic disturbances associated with cardiovascular events in coronary artery disease. *Nature Communications,15*(1), 5729. https://doi.org/10.1038/s41467-024-50125-2

Mattes, W., Davis, K., Fabian, E., Greenhaw, J., Herold, M., Looser, R., Mellert, W., Groeters, S., Marxfeld, H., Moeller, N., Montoya-Parra, G., Prokoudine, A., van Ravenzwaay, B., Strauss, V., Walk, T., & Kamp, H. (2014). Detection of hepatotoxicity potential with metabolite profiling (metabolomics) of rat plasma. *Toxicology Letters,230*(3), 467–478. https://doi.org/10.1016/j.toxlet.2014.07.021

Mayers, J. R., Torrence, M. E., Danai, L. V., Papagiannakopoulos, T., Davidson, S. M., Bauer, M. R., Lau, A. N., Ji, B. W., Dixit, P. D., & Hosios, A. M. (2016). Tissue of origin dictates branched-chain amino acid metabolism in mutant Kras-driven cancers. *Science,353*(6304), 1161–1165.

McAllister, S. S., & Weinberg, R. A. (2010). Tumor-host interactions: A far-reaching relationship. *Journal of Clinical Oncology,28*(26), 4022–4028. https://doi.org/10.1200/JCO.2010.28.4257

Mercuro, G., Cadeddu, C., Piras, A., Dessì, M., Madeddu, C., Deidda, M., Serpe, R., Massa, E., & Mantovani, G. (2007). Early epirubicin-induced myocardial dysfunction revealed by serial tissue doppler echocardiography: Correlation with inflammatory and oxidative stress markers. *The Oncologist,12*(9), 1124–1133. https://doi.org/10.1634/theoncologist.12-9-1124

Mohammed, S., Shamseddine, A. A., Newcomb, B., Chavez, R. S., Panzner, T. D., Lee, A. H., Canals, D., Okeoma, C. M., Clarke, C. J., & Hannun, Y. A. (2021). Sublethal doxorubicin promotes migration and invasion of breast cancer cells: Role of Src family non-receptor tyrosine kinases. *Breast Cancer Research,23*(1), 76. https://doi.org/10.1186/s13058-021-01452-5

Monsuez, J. J. (2012). Detection and prevention of cardiac complications of cancer chemotherapy. *Archives of Cardiovascular Diseases,105*(11), 593–604. https://doi.org/10.1016/j.acvd.2012.04.008

Moses, M. A., & Neckers, L. (2015). The GLU that holds cancer together: Targeting GLUtamine transporters in breast cancer. *Cancer Cell,27*(3), 317–319.

Niu, Q. Y., Li, Z. Y., Du, G. H., & Qin, X. M. (2016). (1)H NMR based metabolomic profiling revealed doxorubicin-induced systematic alterations in a rat model. *Journal of Pharmaceutical and Biomedical Analysis,118*, 338–348. https://doi.org/10.1016/j.jpba.2015.10.026

Palaskas, N. L., Segura, A., Lelenwa, L., Siddiqui, B. A., Subudhi, S. K., Lopez-Mattei, J., Durand, J. B., Deswal, A., Zhao, B., Maximilian Buja, L., & Iliescu, C. (2021). Immune checkpoint inhibitor myocarditis: Elucidating the spectrum of disease through endomyocardial biopsy. *European Journal of Heart Failure,23*(10), 1725–1735. https://doi.org/10.1002/ejhf.2265

Pang, Z., Chong, J., Zhou, G., de Lima Morais, D. A., Chang, L., Barrette, M., Gauthier, C., Jacques, P., Li, S., & Xia, J. (2021). MetaboAnalyst 5.0: Narrowing the gap between raw spectra and functional insights. *Nucleic Acids Research,49*, W388–W396. https://doi.org/10.1093/nar/gkab382

Patti, G. J., Yanes, O., & Siuzdak, G. (2012). Innovation: metabolomics: The apogee of the omics trilogy. *Nature Reviews Molecular Cell Biology,13*(4), 263–269. https://doi.org/10.1038/nrm3314

Planek, M. I. C., Manshad, A., Hein, K., Hemu, M., Ballout, F., Varandani, R., Venugopal, P., & Okwuosa, T. (2020). Prediction of doxorubicin cardiotoxicity by early detection of subclinical right ventricular dysfunction. *Cardio-Oncology,6*(1), 10. https://doi.org/10.1186/s40959-020-00066-8

Pravenec, M., Silhavy, J., Zidek, V., Mlejnek, P., Landa, V., Simakova, M., Strnad, H., Oliyarnyk, O., Kazdova, L., & Kurtz, T. W. (2014). Fumaric acid esters can block pro-inflammatory actions of human CRP and ameliorate metabolic disturbances in transgenic spontaneously hypertensive rats. *Atherosclerosis,235*(2), Article e268. https://doi.org/10.1016/j.atherosclerosis.2014.05.802

Qin, C., Murali, S., Lee, E., Supramaniam, V., Hausenloy, D. J., Obungoloch, J., Brecher, J., Lin, R., Ding, H., Akudjedu, T. N., Anazodo, U. C., Jagannathan, N. R., Ntusi, N. A. B., Simonetti, O. P., Campbell-Washburn, A. E., Niendorf, T., Mammen, R., & Adeleke, S. (2022). Sustainable low-field cardiovascular magnetic resonance in changing healthcare systems. *European Heart Journal. Cardiovascular Imaging,23*(6), e246–e260. https://doi.org/10.1093/ehjci/jeab286

QuanJun, Y., GenJin, Y., LiLi, W., YongLong, H., Yan, H., Jie, L., JinLu, H., Jin, L., Run, G., & Cheng, G. (2017). Protective effects of dexrazoxane against doxorubicin-induced cardiotoxicity: A metabolomic study. *PLoS ONE,12*(1), Article e0169567. https://doi.org/10.1371/journal.pone.0169567

Rahman, A. M., Yusuf, S. W., & Ewer, M. S. (2007). Anthracycline-induced cardiotoxicity and the cardiac-sparing effect of liposomal formulation. *International Journal of Nanomedicine,2*(4), 567–583.

Rushing, B. R., Molina, S., & Sumner, S. (2023). Metabolomics analysis reveals altered metabolic pathways and response to doxorubicin in drug-resistant triple-negative breast cancer cells. *Metabolites,13*(7), 865.

Saidi, A., & Alharethi, R. (2011). Management of chemotherapy induced cardiomyopathy. *Current Cardiology Reviews,7*(4), 245–249. https://doi.org/10.2174/157340311799960681

Schnackenberg, L. K., Pence, L., Vijay, V., Moland, C. L., George, N., Cao, Z., Yu, L. R., Fuscoe, J. C., Beger, R. D., & Desai, V. G. (2016). Early metabolomics changes in heart and plasma

during chronic doxorubicin treatment in B6C3F1 mice. *Journal of Applied Toxicology,36*(11), 1486–1495. https://doi.org/10.1002/jat.3307

Schulze, P. C., Drosatos, K., & Goldberg, I. J. (2016). Lipid use and misuse by the heart. *Circulation Research,118*(11), 1736–1751. https://doi.org/10.1161/CIRCRESAHA.116.306842

Singal, P. K., & Iliskovic, N. (1998). Doxorubicin-induced cardiomyopathy. *New England Journal of Medicine,339*(13), 900–905.

Sivakumar, R., Babu, P. V. A., & Shyamaladevi, C. S. (2008). Protective effect of aspartate and glutamate on cardiac mitochondrial function during myocardial infarction in experimental rats. *Chemico-Biological Interactions,176*(2–3), 227–233.

Sivakumar, R., Babu, P. V. A., & Shyamaladevi, C. S. (2011). Aspartate and glutamate prevents isoproterenol-induced cardiac toxicity by alleviating oxidative stress in rats. *Experimental and Toxicologic Pathology,63*(1–2), 137–142.

Srivastava, S. (2019). Emerging Insights into the metabolic alterations in aging using metabolomics. *Metabolites,9*(12), 301.

Strigun, A., Wahrheit, J., Beckers, S., Heinzle, E., & Noor, F. (2011). Metabolic profiling using HPLC allows classification of drugs according to their mechanisms of action in HL-1 cardiomyocytes. *Toxicology and Applied Pharmacology,252*(2), 183–191. https://doi.org/10.1016/j.taap.2011.02.008

Takemura, G., & Fujiwara, H. (2007). Doxorubicin-induced cardiomyopathy from the cardiotoxic mechanisms to management. *Progress in Cardiovascular Diseases,49*(5), 330–352. https://doi.org/10.1016/j.pcad.2006.10.002

Tan, G., Lou, Z., Liao, W., Zhu, Z., Dong, X., Zhang, W., Li, W., & Chai, Y. (2011). Potential biomarkers in mouse myocardium of doxorubicin-induced cardiomyopathy: A metabonomic method and its application. *PLoS ONE,6*(11), Article e27683. https://doi.org/10.1371/journal.pone.0027683

Thonusin, C., Nawara, W., Arinno, A., Khuanjing, T., Prathumsup, N., Ongnok, B., Chattipakorn, S. C., & Chattipakorn, N. (2023a). Effects of melatonin on cardiac metabolic reprogramming in doxorubicin-induced heart failure rats: A metabolomics study for potential therapeutic targets. *Journal of Pineal Research,75*(1), Article e12884. https://doi.org/10.1111/jpi.12884

Thonusin, C., Nawara, W., Khuanjing, T., Prathumsup, N., Arinno, A., Ongnok, B., Arunsak, B., Sriwichaiin, S., Chattipakorn, S. C., & Chattipakorn, N. (2023b). Blood metabolomes as non-invasive biomarkers and targets of metabolic interventions for doxorubicin and trastuzumab-induced cardiotoxicity. *Archives of Toxicology,97*(2), 603–618. https://doi.org/10.1007/s00204-022-03412-0

Thonusin, C., Osataphan, N., Leemasawat, K., Nawara, W., Sriwichaiin, S., Supakham, S., Gunaparn, S., Apaijai, N., Somwangprasert, A., Phrommintikul, A., Chattipakorn, S. C., & Chattipakorn, N. (2024). Changes in blood metabolomes as potential markers for severity and prognosis in doxorubicin-induced cardiotoxicity: A study in HER2-positive and HER2-negative breast cancer patients. *Journal of Translational Medicine,22*(1), 398. https://doi.org/10.1186/s12967-024-05088-9

Totzeck, M., Aide, N., Bauersachs, J., Bucerius, J., Georgoulias, P., Herrmann, K., Hyafil, F., Kunikowska, J., Lubberink, M., Nappi, C., Rassaf, T., Saraste, A., Sciagra, R., Slart, R., Verberne, H., & Rischpler, C. (2023). Nuclear medicine in the assessment and prevention of cancer therapy-related cardiotoxicity: Prospects and proposal of use by the European Association of Nuclear Medicine (EANM). *European Journal of Nuclear Medicine and Molecular Imaging,50*(3), 792–812. https://doi.org/10.1007/s00259-022-05991-7

Van Geldermalsen, M., Wang, Q., Nagarajah, R., Marshall, A., Thoeng, A., Gao, D., Ritchie, W., Feng, Y., Bailey, C., & Deng, N. (2016). ASCT2/SLC1A5 controls glutamine uptake and tumour growth in triple-negative basal-like breast cancer. *Oncogene,35*(24), 3201–3208.

Vejpongsa, P., & Yeh, E. T. (2014). Prevention of anthracycline-induced cardiotoxicity: Challenges and opportunities. *Journal of the American College of Cardiology,64*(9), 938–945. https://doi.org/10.1016/j.jacc.2014.06.1167

Verheijen, M., Schrooders, Y., Gmuender, H., Nudischer, R., Clayton, O., Hynes, J., Niederer, S., Cordes, H., Kuepfer, L., Kleinjans, J., & Caiment, F. (2018). Bringing in vitro analysis closer to in vivo: Studying doxorubicin toxicity and associated mechanisms in 3D human microtissues with PBPK-based dose modelling. *Toxicology Letters,294*, 184–192. https://doi.org/10.1016/j.toxlet.2018.05.029

Viant, M. R., Ebbels, T. M. D., Beger, R. D., Ekman, D. R., Epps, D. J. T., Kamp, H., Leonards, P. E. G., Loizou, G. D., MacRae, J. I., van Ravenzwaay, B., Rocca-Serra, P., Salek, R. M., Walk, T., & Weber, R. J. M. (2019). Use cases, best practice and reporting standards for metabolomics in regulatory toxicology. *Nature Communications,10*(1), 3041. https://doi.org/10.1038/s41467-019-10900-y

Volkova, M., & Russell, R., 3rd. (2011). Anthracycline cardiotoxicity: Prevalence, pathogenesis and treatment. *Current Cardiology Reviews,7*(4), 214–220.

Wang, X., Gao, Y., Tian, Y., Liu, X., Zhang, G., Wang, Q., Xie, W., Liu, K., Qian, Q., & Wang, Q. (2020). Integrative serum metabolomics and network analysis on mechanisms exploration of Ling–Gui–Zhu–Gan decoction on doxorubicin-induced heart failure mice. *Journal of Ethnopharmacology,250*, Article 112397. https://doi.org/10.1016/j.jep.2019.112397

Watanabe, K., Nagao, M., Toh, R., Irino, Y., Shinohara, M., Iino, T., Yoshikawa, S., Tanaka, H., Satomi-Kobayashi, S., Ishida, T., & Hirata, K.-I. (2021). Critical role of glutamine metabolism in cardiomyocytes under oxidative stress. *Biochemical and Biophysical Research Communications,534*, 687–693. https://doi.org/10.1016/j.bbrc.2020.11.018

Wen, J. X., Li, R. S., Wang, J., Hao, J. J., Qin, W. H., Yang, T., Wang, R. L., Wei, S. Z., Liu, X. Y., Li, H. T., Wang, J. B., Liu, H. H., & Zhao, Y. L. (2020c). Therapeutic effects of aconiti lateralis radix praeparata combined with Zingiberis Rhizoma on doxorubicin-induced chronic heart failure in rats based on an integrated approach. *Journal of Pharmacy and Pharmacology,72*(2), 279–293. https://doi.org/10.1111/jphp.13191

Wen, J., Ma, X., Niu, M., Hao, J., Huang, Y., Wang, R., Li, R., Wang, J., & Zhao, Y. (2020a). Metabolomics coupled with integrated approaches reveal the therapeutic effects of higenamine combined with [6]-gingerol on doxorubicin-induced chronic heart failure in rats. *Chinese Medicine,15*(1), 120. https://doi.org/10.1186/s13020-020-00403-0

Wen, J., Zhang, L., Wang, J., Wang, J., Wang, L., Wang, R., Li, R., Liu, H., Wei, S., Li, H., Zou, W., & Zhao, Y. (2020b). Therapeutic effects of higenamine combined with [6]-gingerol on chronic heart failure induced by doxorubicin via ameliorating mitochondrial function. *Journal of Cellular and Molecular Medicine,24*(7), 4036–4050. https://doi.org/10.1111/jcmm.15041

Würtz, P., Havulinna, A. S., Soininen, P., Tynkkynen, T., Prieto-Merino, D., Tillin, T., Ghorbani, A., Artati, A., Wang, Q., & Tiainen, M. (2015). Metabolite profiling and cardiovascular event risk: A prospective study of 3 population-based cohorts. *Circulation,131*(9), 774–785.

Xue, Z., Zhuo, L., Zhang, B., Zhu, L., Xiang, X., Zhang, C., Liu, W., Tan, G., & Liao, W. (2023). Untargeted metabolomics reveals the combination effects and mechanisms of Huangqi-fuzi herb-pair against doxorubicin-induced cardiotoxicity. *Journal of Ethnopharmacology,305*, Article 116109. https://doi.org/10.1016/j.jep.2022.116109

Yeh, E. T., & Bickford, C. L. (2009). Cardiovascular complications of cancer therapy: Incidence, pathogenesis, diagnosis,

and management. *Journal of the American College of Cardiology,53*(24), 2231–2247. https://doi.org/10.1016/j.jacc.2009.02.050

Yi, X., Zhu, J., Zhang, J., Gao, Y., Chen, Z., Lu, S., Cai, Z., Hong, Y., & Wu, Y. (2018). Investigation of the reverse effect of Danhong injection on doxorubicin-induced cardiotoxicity in H9c2 cells: Insight by LC-MS based non-targeted metabolomic analysis. *Journal of Pharmaceutical and Biomedical Analysis,152*, 264–270. https://doi.org/10.1016/j.jpba.2018.02.012

Yoo, H. C., Yu, Y. C., Sung, Y., & Han, J. M. (2020). Glutamine reliance in cell metabolism. *Experimental & Molecular Medicine,52*(9), 1496–1516.

Yu, L. R., Cao, Z., Makhoul, I., Daniels, J. R., Klimberg, S., Wei, J. Y., Bai, J. P., Li, J., Lathrop, J. T., Beger, R. D., & Todorova, V. K. (2018). Immune response proteins as predictive biomarkers of doxorubicin-induced cardiotoxicity in breast cancer patients. *Experimental Biology and Medicine (Maywood, N.J.),243*(3), 248–255. https://doi.org/10.1177/1535370217746383

Yuan, Y., Fan, S., Shu, L., Huang, W., Xie, L., Bi, C., Yu, H., Wang, Y., & Li, Y. (2020). Exploration the mechanism of doxorubicin-induced heart failure in rats by integration of proteomics and metabolomics data. *Frontiers in Pharmacology,11*, Article 600561. https://doi.org/10.3389/fphar.2020.600561

Yun, W., Qian, L., Yuan, R., & Xu, H. (2021). Periplocymarin alleviates doxorubicin-induced heart failure and excessive accumulation of ceramides. *Frontiers in Cardiovascular Medicine,8*, Article 732554. https://doi.org/10.3389/fcvm.2021.732554

Zhang, Y., Zhang, M., Zhu, W., Yu, J., Wang, Q., Zhang, J., Cui, Y., Pan, X., Gao, X., & Sun, H. (2020). Succinate accumulation induces mitochondrial reactive oxygen species generation and promotes status epilepticus in the kainic acid rat model. *Redox Biology,28*, Article 101365. https://doi.org/10.1016/j.redox.2019.101365

Zhang, Y., Zhou, Q., Ding, X., Wang, H., & Tan, G. (2021). HILIC-MS-based metabolomics reveal that Astragalus polysaccharide alleviates doxorubicin-induced cardiomyopathy by regulating sphingolipid and glycerophospholipid homeostasis. *Journal of Pharmaceutical and Biomedical Analysis,203*, Article 114177. https://doi.org/10.1016/j.jpba.2021.114177

Zhao, L. K., Zhao, Y. B., & Zhang, P. X. (2021). High-throughput metabolomics discovers metabolite biomarkers and insights the protective mechanism of schisandrin B on myocardial injury rats. *Journal of Separation Science,44*(3), 717–725. https://doi.org/10.1002/jssc.202000875

Zheng, G., Zheng, M., Yang, B., Fu, H., & Li, Y. (2019). Improving breast cancer therapy using doxorubicin loaded solid lipid nanoparticles: Synthesis of a novel arginine-glycine-aspartic tripeptide conjugated, pH sensitive lipid and evaluation of the nanomedicine in vitro and in vivo. *Biomedicine & Pharmacotherapy,116*, Article 109006. https://doi.org/10.1016/j.biopha.2019.109006

Zhou, Q., Meng, P., Zhang, Y., Chen, P., Wang, H., & Tan, G. (2020). The compatibility effects of sini decoction against doxorubicin-induced heart failure in rats revealed by mass spectrometry-based serum metabolite profiling and computational analysis. *Journal of Ethnopharmacology,252*, Article 112618. https://doi.org/10.1016/j.jep.2020.112618